Department of Pathology & Immunology
Baylor College of Medicine

Trainee Research Symposium

April 12, 2024

8:00 am - 1:15 pm

Cullen Auditorium, Rayzor Lounge
1 Baylor Plaza, Houston, TX 77030

Join from PC, Mac, Linux, iOS or Android: https://bcm.zoom.us/j/92563512024?pwd=Sk5CMXZyUDVobmQxNkFRcHM5OG1GZz09
Password: 716626

Program

7:30 - 8:00 am	**Breakfast**
8:00 - 8:10 am	**Welcome and Opening Remarks** **Jun Teruya, MD, DSc**
8:10-9:10 am	**Oral Trainee Presentations: Session 1** **Moderator: William Decker, PhD** **Anil K. Chokkalla, PhD** **Nicholas J. Dcunha, MBBS, MD** **Zian Liao, MBBS, MS** **Anil K. Devakrishnan, PhD**
9:10-10:10 am	**Faculty Presentations** **Moderator: Sridevi Devaraj, PhD, DABCC, FRSC** **Melissa M. Blessing, DO** *"Taking Autopsy Research to the Next Level: Oncologic and Forensic Collaboration"* **Juan Vitelio Rodriguez, MD, FASCP** *"New Kids on the Block – Is the Standard of Care for TTP Shifting?"* **Daniel Lacorazza, PhD** *"Development of Targeted Therapy in Pediatric Leukemia"*
10:10-10:20 am	**Break**
10:20 - 11:20 am	**Oral Trainee Presentations: Session 2** **Moderator: Angshumoy Roy, MBBS, PhD** **Belkys Sanchez, MS, PhD** **Dilshad Dhaliwal, MD** **Sharon B. Amanya** **Komal K. Bollepogu Raja, PhD**
11:20am-12:05 pm	**Keynote Lecture** **Jason T. Huse, MD, PhD** *"Characterizing and Targeting Epigenetic Dysfunction in Brain Cancer"*
12:05 -1:05 pm	**Poster Session and Lunch** **Boxed lunch will be provided**
1:05 - 1:15 pm	**Awards Session and Closing Remarks** **Martin M. Matzuk, MD, PhD and James Versalovic, MD, PhD**

Trainee Research Committee: Drs. Thomas A. Cooper, Choladda V. Curry, William Decker, Sridevi Devaraj, Sagar Dhamne, Ashley Holloman, Martin M. Matzuk, Angshumoy Roy, and Jun Teruya, Chief Residents (Drs. Eltahir and Platero) and Associate Chief Residents (Drs. Dodson and Huffman)

Keynote Lecture

"Characterizing and Targeting Epigenetic Dysfunction in Brain Cancer"

Jason T. Huse, MD, PhD

Professor
Departments of Pathology and Translational Molecular Pathology
Section Chief, Neuropathology
University of Texas MD Anderson Cancer Center

Faculty Presentations

Clinical Faculty (AP)

"Taking Autopsy Research to the Next Level: Oncologic and Forensic Collaboration"

Melissa M. Blessing, DO

Medical Director of Autopsy Service
Neuropathology and Pediatric Pathology
Anatomic Pathology QA/Safety Liaison
Texas Children's Hospital
Assistant Professor of Pathology & Immunology
Baylor College of Medicine

Clinical Faculty (CP)

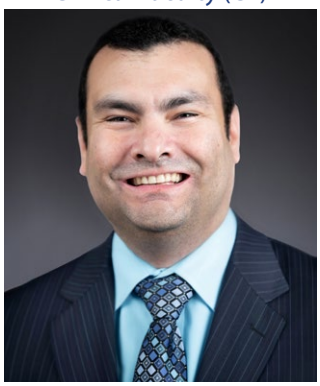

"New Kids on the Block – Is the Standard of Care for TTP Shifting?"

Juan Vitelio Rodriguez, MD, FASCP

Transfusion Medicine & Coagulation
Texas Children's Hospital
Assistant Professor of Pathology & Immunology
Baylor College of Medicine

Research Faculty

"Development of Targeted Therapy in Pediatric Leukemia"

Daniel Lacorazza, PhD

Principal Investigator, Experimental
Immunology & Hematology
Texas Children's Hospital
Associate Professor of Pathology & Immunology and Pediatrics
Baylor College of Medicine

Trainee Presentation Abstracts

Trainee Poster Presentation Abstracts

Trainee Poster Presentation Abstracts

Path Towards Biopsy-Free Diagnosis of Celiac Disease in Pediatric Patients

Anil K Chokkalla[1,2], Meg M Parham[1,2], Douglas S Fishman[3] and Sridevi Devaraj[1,2]

[1]Department of Pathology & Immunology, Baylor College of Medicine, Houston, TX, USA
[2]Department of Pathology, Texas Children's Hospital, Houston, TX, USA
[3]Division of Pediatric Gastroenterology, Hepatology and Nutrition, Department of Pediatrics, Baylor College of Medicine and Texas Children's Hospital, Houston, Texas, USA

Introduction: Diagnosis of celiac disease in children involves integrated evaluation of clinical presentation, serology testing, genetic susceptibility testing and duodenal biopsy examination. The 2023 American College of Gastroenterology evidence-based guidelines recommend a biopsy-free approach utilizing tissue transglutaminase antibody titers >10 times upper limit of normal and subsequent endomysial antibody seropositivity as sufficient for diagnosis of celiac disease in children, without the need for invasive duodenal biopsy. The objective of this study is to assess the diagnostic accuracy of biopsy-free approach at our large pediatric center.
Methods: We conducted a retrospective cohort study involving pediatric patients who underwent biopsy-based histological evaluation for the confirmation of CD diagnosis between May 2019 and May 2023. For these patients, the tissue transglutaminase and endomysial antibody test results were retrieved from the electronic medical records. Performance of the biopsy-free approach was assessed using the duodenal histology as the gold standard for celiac disease diagnosis.
Results: Tissue transglutaminase antibody titers >10 times upper limit of normal alone demonstrated a diagnostic accuracy of 73%, sensitivity of 65%, and specificity of 98%, with a positive predictive value of 99% and negative predictive value of 44% for identifying pediatric patients with celiac disease. Endomysial antibody testing is underutilized at our center. Biopsy-free approach yielded a similar diagnostic accuracy in pediatric patients with pre-existing type 1 diabetes mellitus.
Conclusions: Positive predictive value of tissue transglutaminase antibody titers >10x upper limit of normal is sufficiently high for diagnosis of celiac disease in children, and may allow for deferral of duodenal biopsy at diagnosis.

Trainee Presentation Abstracts

Multi-Aminoacyl tRNA Synthetase Complex-mediated Sensing of Antigen Homology Dictates mTORC1-dependent T_H1 Polarization in Dendritic Cells

Sharon Bright Amanya[1,2], Arnav Murthy[3], Vanaja Konduri[1,4,&5], & William K. Decker[1,4,&5]

[1] Department of Pathology and Immunology; [2]Graduate School of Biomedical Sciences; Baylor College of Medicine; [3] Department of natural sciences, Rice University; [4]Dan L. Duncan Comprehensive Cancer Center, Baylor College of Medicine; [5]Center for Cell and Gene Therapy, Baylor College of Medicine, Houston, Texas 77030

Introduction: Type 1 T-helper immune polarization is critical to the formation of durable antitumor immunity. Therefore, therapies that initiate or enhance type 1 (T_H1) immune responses are the next frontier in cancer immunotherapy. While the dendritic cell (DC) is central to the initiation, direction, and regulation of T_H1 immunity, the exploitation of this cell type for cancer immunotherapy has been minimal, largely because the mechanisms that regulate DC facilitation of T_H1 polarization remain to be fully understood. We have previously described a novel strategy for T_H1 polarization of DC in which the homology of antigenic epitopes plays a critical role. When bound MHC class I and II peptide epitopes share an identical stretch of at least 5 amino acids, this homology is sufficient to drive robust T_H1 polarization, rendering manipulation of this mechanism an attractive target for cancer immunotherapy. This study explores the mechanisms for antigen homology sensing and the downstream signaling pathways that mediate T_H1 polarization.

Methods: We used both primary human cells (monocyte derived DCs isolated from blood of healthy donors) and mouse models to address the research questions. A wide range of experimental methods were employed including mass spectrometry, reverse phase protein array, co-immunoprecipitation, western blot, chromatin immunoprecipitation, PCR and ELISA to study the sensing of homologous antigens as well as the downstream signaling pathways they regulate in DCs.

Results: Using mass spectrometry, we identified that MHC molecules interact with the multi-aminoacyl tRNA synthetase (mARS) complex, a multi-subunit protein complex comprised of aminoacyl tRNA synthetases (aaRS) and interacting proteins(AIMPs). Further, the composition of aaRS within the complex undergoes changes consistent with amino acids present in the homologous MHC peptides; suggesting a sensing role. Knockout of AIMP1, a critical scaffold of the mARS complex revealed the mechanistic target of rapamycin complex 1 (mTORC1) pathway as a significant downstream effector that's inhibited following homologous antigen loading. Accordingly, Co-IP showed a direct interaction of the mARS with Rags, small G proteins known to transmit signals from amino acid sensors to the mTORC1 complex. Consistent with the known regulation of *IL12*/*IL10* axis by mTORC1 via NFkB, ChIP PCR showed significantly high binding of NFκB to the *IL12* promoter and a reduction in *IL10* promoter binding in DC loaded with homologous antigens. Additionally, IL-12 was significantly upregulated with concomitant reduction of IL-10.

Conclusion: These findings describe the intricacies of a novel mechanism through which T_H1 polarization in DC is governed by the homology of MHC peptide epitopes sensed by the mARS complex. Further delineation of this complex mechanism will be of paramount importance to the identification of specific, druggable targets, the manipulation of which will enhance therapeutic outcomes in cancer immunotherapy.

Clinical Performance of the BIOFIRE® Joint Infection Multiplex PCR Panel for Pathogen Identification in Joint and Pleural Fluids from Pediatric Patients

Belkys C. Sánchez[1,2], Hadi Sayeed[2], Denver T. Niles[1,2], James J. Dunn[1,2]

[1]Department of Pathology & Immunology, Baylor College of Medicine, Houston, TX [2]Department of Pathology, Texas Children's Hospital, Houston, TX

Introduction

The isolation and identification of microbial pathogens in sterile body fluids from children poses challenges. Specimen volume may be limited and microbial burden low. Pre-treatment with antimicrobials can render the pathogen non-viable in culture. In such cases, and with fastidious organisms like *Kingella kingae*, molecular methods are useful for identification of the causative agent. We evaluated the clinical performance of the bioMérieux BIOFIRE® Joint Infection Panel (JIP) to standard-of-care (SOC) diagnostic techniques applied to joint/bone and pleural fluids from pediatric patients.

Methods

One hundred-thirty six specimens (77 joint/bone and 59 pleural fluids) archived at -80ºC were tested. Specimens had been previously tested by a lab-developed real-time PCR assay (LDT PCR), routine culture, and/or reference 16s rRNA PCR and sequencing. The LDT PCR assay includes primers and probes specific for *S. aureus*, methicillin resistance (*mec*A), *K. kingae*, *S. pneumoniae*, *S. pyogenes* and *N. meningitidis*. Specimen aliquots were thawed, vortexed and tested using the JIP per the manufacturer's instructions. Two-by-two data tables were used to determine agreement between the JIP and SOC testing results.

Results

The JIP identified a pathogen in 56 out of 62 joint fluids positive by SOC testing, with a positive percent agreement (PPA) of 90.3%. False negatives with the JIP were detected in the LDT PCR with cycle thresholds (Cts) ≥36.4 and included one *K. kingae*, one MSSA, one MRSA, and one *S. pyogenes*. One specimen in which *S. anginosus* was recovered in broth culture only, and one specimen positive for *N. gonorrhoeae* by 16s rRNA PCR and sequencing were also negative by the JIP. Two false positives were observed with joint fluids; one *Peptoniphilus* and one *E. coli*, which were not detected by SOC testing. The JIP identified a pathogen in 37 out of 40 pleural fluids positive by SOC testing (PPA=92.5%). MSSA, MRSA, and *S. pneumoniae* were identified in three different samples by LDT PCR (Cts ≥35.6) but not detected by the JIP. Five false positives were identified with the JIP; one *Parvimonas micra*, two *H. influenzae*, one *S. pyogenes,* and one *Streptococcus* spp. The JIP had good negative percent agreement (91.3%) compared to SOC techniques for joint fluids but not for pleural fluids (81.5%).

Conclusions

The JIP testing showed an overall 87.5% concordance rate with SOC testing across both types of samples. While the JIP demonstrated a strong ability to identify true positives (PPA=91.2%), its ability to rule out infection was lower than expected (NPA=86%). This was in part due to detection of respiratory flora by the JIP in pleural fluids that were not isolated by culture. Despite this, the JIP holds promise for influencing treatment decisions in children, especially in culture negative cases. Further evaluation of this test is warranted.

Discovery and Characterization of Small Molecule Drugs to Target Estrogen Receptor Mutants in Breast Cancer

Anil Kumar Devakrishnan, Ramkumar Modukuri, Suzanne A W Fuqua and Martin M. Matzuk and Murugesan Palaniappan[#]

Background:
The acquisition of estrogen receptor alpha (ERα) gene (*ESR1*) mutations is a key driver for the development of resistance to current endocrine therapy in breast cancer. Clinical studies have shown that *ESR1* mutations are frequently observed in metastatic ER-positive breast cancer patients and are associated with poor survival. It is well appreciated that activating *ESR1* somatic mutations, especially Y537S and D538G, can drive estrogen-independent activities. In addition, these *ESR1* mutations diminish the potency of the current standard-of-care agents (tamoxifen and fulvestrant) that bind ERα directly. Therefore, it is a critical need to develop next-generation antiestrogens that inhibit ERα mutant signaling in breast cancer to improve patient survival. Here, we search for small molecule inhibitors against ERα mutants Y537S and D538G using DNA-encoded chemical library (DECL) selections.

Methods:
ERα ligand binding domain (LBD) proteins corresponding to wild type (WT), Y537S and D538G mutants were expressed in *E. coli* and purified by Ni-NTA, anion exchange, and size exclusion chromatography. The ability of these purified proteins to bind ligands was tested in biochemical assays to validate their use in DECL selections. We conducted a DNA-encoded chemical library affinity selection using our in-house collection of 6 billion compounds against WT, Y537S and D538G mutants ER ligand binding domain (LBD) proteins in the presence and absence of estradiol. Hits that enriched with these targets were resynthesized off-DNA and tested in biochemical assays. We have performed functional studies with these compounds in wildtype and CRISPR-Cas9 knock-in Y537S or D538G mutant MCF-7 and T47D breast cancer cells.

Results: We have successfully purified microgram amounts of ERα LBD for WT, Y537S, and D538G proteins. The ability of these purified proteins to bind ligands was tested using homogeneous time-resolved fluorescence and fluorescent polarization assays. SRC3 peptide binds to the WT ERα LBD in the presence of estradiol, whereas Y537S and D538G LBDs bind the SRC3 peptide in the absence of estradiol, consistent with these mutants constitutively binding to SRC3. Our multibillion small molecule collections of DNA-encoded chemical library screen identified several hits in WT and mutant ERα LBDs. To confirm the selection output, we synthesized off-DNA compounds and validated these in biochemical and cell-based studies. Compounds CDD-1274, CDD-1802 and CDD-3209 dramatically decrease the WT and mutant ERα protein levels in many cell types. These compounds greatly reduce protein levels for GREB1, TFF1, c-MYC, E2F1, and survivin in wildtype and mutant breast cancer cells, and they increase levels of p21 and cleaved PARP, a marker for apoptosis in wildtype and mutant ER positive breast cancer cells but not in ER negative breast cancer cells.

Conclusions:
We have identified potent novel ERα mutant binders using our DNA-encoded chemical library platform. Our compounds are active in biochemical and ERα mutant cell lines, suggesting these molecules are potential chemical probes to explore in *in vivo* models of breast cancer. In a panel of ER+ breast cancer cell lines were sensitive to CDD-1274, CDD-1802 and CDD-3209, whereas

ER- cell lines tested were insensitive. Furthermore, our study rapidly identified novel WT and mutants ERα degrader lead compounds from DNA-encoded chemical library screening with minimal medicinal chemistry efforts.

Trainee Presentation Abstracts

TITLE: Is Mitotic count in GIST (Gastrointestinal Stromal Tumor) stomach biopsies significant for patient care? A tertiary hospital care experience

AUTHORS: Dilshad Dhaliwal[1], Tamadar Al-Doheyan[1], Peyman Dinarvand[1], E. Celia Marginean[1], Tannaz Armaghany[2], Shilpa Jain[1]

[1]Department of Pathology & Immunology; Baylor College of Medicine, [2] Department of Medicine - Hematology & Oncology

Introduction:

GIST are the most common mesenchymal tumors of the gastrointestinal tract. They are derived from activating mutations of *KIT* or *PDGFRA* genes. The primary treatment is surgery; however, tyrosine kinase inhibitors are given neoadjuvant or adjuvant for aggressive tumors. Although the risk of progressive disease is based on location, mitoses, and tumor size, reporting of mitotic count on diagnostic biopsies is debatable and its role in patient management is still unclear.

Method:

We performed a retrospective review and analysis of clinicopathologic data and clinical management of 78 consecutive stomach GIST from 2019-2023. The risk stratification in biopsies was compared with resection specimens where available. The rationale behind all GIST that received neoadjuvant therapy was assessed.

Results:

Of 78 patients with stomach GIST (M: F ratio 1.6:1, age 38-82), mitotic count and risk stratification concordance were assessed in biopsies and resections. Among 65 untreated cases, 69.2% (45/65) had diagnostic biopsies; of these, in 46.4% (21/45) mitotic count was reported, 95% low risk (<5/5mm²). Two cases were non-concordant, changing from low to high risk from biopsy to resection. The majority of cases 80.9% (17/21) showed concordant risk stratification between biopsy and resections. Of the 13/78 (16.6 %) cases that had neoadjuvant therapy the rationale for therapy was primarily to reduce the size of the tumor to achieve negative resection margins in 69.2% (9/13) cases; and the critical location of the tumor in 30.7% (4/13) cases. Of these, only 23% (3/13) of GIST were assessed as high risk on preoperative biopsies.

Conclusion:

Current guidelines (CAP for GIST biopsies) require reporting of mitoses and necrosis. Our study, limited by a low number of cases, showed there was no significant difference in the risk stratification between biopsy and resection specimens (p = 0.96). The decision of neoadjuvant treatment was primarily based on tumor location and to decrease tumor burden to achieve R0 resection. Thus, we suggest that mitoses in GIST biopsies should be reported cautiously, only in cases that have at least 5mm^2 of the tumor. Moreover, biopsies may not be representative of the entire tumor, and risk stratification is more accurate on resections.

DICER1 Mutated Mesenchymal Tumors from Different Anatomical Sites Share Morphological, Genomic and Epigenomic Signatures.

Nicholas J Dcunha[1], Maryam Shafiekhani[1], Horatiu Voicu[1], Ninad Patil[1], Norma Quintanilla[1], Deborah Schady[1], Kevin E. Fisher[1], Dolores Lopez-Terrada[1], Nino Rainusso[1], Frank Lin[1], D. Williams Parsons[1], Melissa Blessing[1], Carrie Mohila[1], Angshumoy Roy[1]

[1]Baylor College of Medicine and Texas Children's hospital, Houston, Tx.

Introduction:

DICER1 encodes an RNA endonuclease central to cellular microRNA processing. Germline and somatic *DICER1* mutations underlie the pathogenesis of *DICER1*-mutated sarcomas/mesenchymal tumors in various anatomical sites, including the brain, kidney, uterus, and lungs. However, despite some shared morphological and genetic features, the relatedness among *DICER1*-mutated sarcomas remains unclear. We retrospectively studied seven cases of *DICER1*-mutated sarcomas from distinct anatomical sites (brain, kidney, and uterus) combining light microscopic and immunohistochemical features with genomic and epigenomic analysis.

Methods:

Cases were identified from pathology archives at Texas Children's Hospital based on diagnosis of 'sarcoma' harboring *DICER1* mutations. Light microscopic and immunohistochemical features were reviewed. Tumor genomic features, including mutations, copy number profiles, and gene fusions were assessed using a next generation sequencing (NGS) panel on all 7 cases. Genome-wide methylation analysis was done on 6 of 7 cases using Illumina EPIC array, and tumors classified based on epigenetic features using a Random Forest prediction model from a published molecular neuropathology brain tumor classifier v12.5 (DKFZ, Heidelberg, Germany).

Results:

Seven cases of *DICER1*-mutated sarcomas from the brain (primary intracranial sarcoma; n=4), kidney (anaplastic sarcoma of kidney; n=1), and uterus (rhabdomyosarcoma; n=2) were identified. The median age at presentation was 8 years (range 2-36 years) with a male-to-female ratio of 1.3. Morphologically, 6 of 7 cases had features of high-grade spindle cell sarcoma. Prominent cytoplasmic eosinophilic globules were evident in two of seven cases, cartilaginous differentiation was evident in one case, rhabdomyomatous differentiation by morphology was seen in four cases. Five of six cases showed diffuse or focal immunopositivity for desmin. Despite morphological heterogeneity, genomic analysis revealed biallelic *DICER1* alterations in all 7 cases, including an RNAase IIIB mutation in one of six hotspot sites (p.E1705K x 3; p.E1813D x

– *continued on page 11*

– *continued from page 10*

2; p.G1809R x1; p.D1810Y x 1) along with a second predicted or likely loss-of-function (LOF) mutation and/or loss of heterozygosity. Median variant allele fractions (VAF) were 45% and 38.5% for hotspot and LOF variants consistent with an initiator event. All cases also showed concomitant MAP Kinase activating mutations (*KRAS*, *PDGFRA*). *TP53* mutations were seen in 5 of 7 cases, and *ATRX* mutations in 2 of 7 cases. Genomic findings helped in confirming or refining the initial pathology diagnosis in 6 out of 7 cases. Remarkably, methylation based DKFZ tumor classifier analysis performed on six tumors from diverse anatomic sites (4 brain, 1 kidney, 1 uterus) all nevertheless showed strong (methylation classifier score of > 0.95) relatedness to the CNS Sarcoma DICER1 methylation class.

Conclusion:

DICER1 mutated sarcomas from different anatomical sites show overlapping morphological features consisting of high-grade spindle cell lesions with myogenic differentiation. These tumors uniformly harbor distinct genomic features of *DICER1* mutations; remarkably, irrespective of anatomic location, all sarcomas share a strong relatedness in epigenetic features. Genomic and epigenetic features can be highly effective diagnostic tools in these tumors.

The *Drosophila onecut* Gene is an Essential Regulator of Photoreceptor Development and Function

Komal Kumar Bollepogu Raja[1], Kelvin Yeung[1], David Li-Kroeger[2], Graeme Mardon[1,3]

[1]Department of Pathology and Immunology, Baylor College of Medicine, One Baylor Plaza, Houston, Texas 77030, USA

[2]Department of Neurology, Baylor College of Medicine, One Baylor Plaza, Houston, Texas 77030, USA

[3]Department of Molecular and Human Genetics, Baylor College of Medicine, One Baylor Plaza, Houston, Texas 77030, USA

Introduction

The Onecut family of transcription factors are expressed in a broad array of tissues and play significant roles in regulating their development, function and maintenance. The three mammalian *onecut* genes contain both a DNA-binding cut domain and a divergent homeodomain and are highly conserved from *Drosophila* to humans. The *onecut* genes activate a number of gene families and are required for proper specification and differentiation of multiple tissue types including the central nervous system, liver, pancreas, retina, as well as playing important roles in a variety of cancers. In mice, the *Onecut* genes are expressed during retinal differentiation and both *Onecut1* and *Onecut2* are required for normal eye development. Removal of either of these genes results in the loss of 50-80% of horizontal cells in the adult eye, while loss of both genes leads to complete loss of horizontal cells and a substantial reduction of other retinal cells such as cone, retinal ganglion, and starburst amacrine cells. However, very little is known about the mechanism of action of the *Onecut* genes and the downstream targets they regulate. *Drosophila* has a single *onecut* ortholog whose DNA-binding cut domain is more than 93% identical to the human *Onecut* homologs. We used *Drosophila* as a model system to decipher the molecular mechanisms of *onecut* function.

Methods

We generated *onecut* null alleles and performed electroretinograms (ERGs) on newly eclosed *onecut* mutant and wild-type adult flies to assay the response to light stimulation. We also performed single cell RNA sequencing (scRNA-seq) from *Drosophila* late larval eye discs of both *onecut* and wild-type flies using the 10x Genomics platform. Both wild-type and mutant sequence data were normalized, scaled and reduced. We then used the Seurat R package to integrate both datasets to identify downregulated genes in *onecut* mutants. Single nuclear assay for transposase accessible chromatin (snATAC) was also performed for wild-type, while Chromatin Immunoprecipitation sequencing (ChIP-seq) was conducted using GFP/3xFLAG-tagged *onecut-BAC* rescued *onecut* null mutant flies. Finally, we used transmission electron microscopy to carry a detailed analysis of *onecut* mutant eyes and brains.

Results

Our results show that *onecut* is required for normal visual system development and function in *Drosophila*. Although the external adult eye appears normal, the internal structure of the eye is

– continued on page 13

– *continued from page 12*

reduced with smaller rhabdomeres, while the supporting pigment cells are significantly larger in size. Similarly, the lamina cartridges are greatly disrupted in the mutant with degenerating photoreceptor axon terminals. Consistent with this data, null mutants are completely unresponsive to light as assayed by ERGs. Phenotypic analyses show that photoreceptor nuclei are displaced proximally throughout the mutant retina. Photoreceptor axon terminals show normal initial projections, however, vestiges of axon terminals are observed in the lamina suggesting failure of correct targeting, thus leading to progressive degeneration. Intersecting our single cell and ChIP-seq datasets, we have identified a list of putative direct and indirect *onecut* targets that is highly enriched for genes already known to play important roles in visual system development and function and likely includes many novel players important in these processes.

Conclusion

Our results suggest that Onecut is an important regulator of photoreceptor development and function in the *Drosophila* eye. Our results are likely to have important implications for human *Onecut* gene function.

Targeting Ephrin Receptor Kinase for the Treatment of Endometriosis, Zian Liao[a,b,c]; Chandrashekhar Madasu[a,b]; Sydney E. Parks[a,b]; Kiran Sharma[a,b]; Kurt M. Bohren[a,b]; Qiuji Ye[a,b]; Feng Li[a,b,d]; Murugesan Palaniappan[a,b]; Zhi Tan[a,b]; Fei Yuan[a,b]; Chad J. Creighton[e,f,g]; Suni Tang[a,b]; Ramya Masand[a,h]; Xiaoming Guan[h]; Damian W. Young[a,b,d]; Diana Monsivais[a,b]; Martin M. Matzuk[a,b,c,d]

[a]Department of Pathology & Immunology, Baylor College of Medicine, Houston, TX, 77030, USA; [b]Center for Drug Discovery, Baylor College of Medicine, Houston, TX, 77030, USA; [c]Department of Molecular and Human Genetics, Baylor College of Medicine, Houston, TX, 77030, USA; [d]Department of Biochemistry and Molecular Pharmacology, Baylor College of Medicine, Houston, TX, 77030, USA; [e]Dan L. Duncan Comprehensive Cancer Center Division of Biostatistics, Baylor College of Medicine, Houston, TX, 77030, [f]Human Genome Sequencing Center, Baylor College of Medicine, Houston, TX, 77030, and [g]Department of Medicine, Baylor College of Medicine, Houston, TX, 77030, [h]Department of Obstetrics and Gynecology, Baylor College of Medicine, Houston, TX, 77030, USA

Introduction:
Endometriosis, defined as the abnormal appearance of endometrial tissues outside of the uterine cavity, is a condition that burdens more than 190 million women globally. Endometriosis not only causes dysmenorrhea and chronic pelvic pain, it also leads to infertility and increased risk for ovarian cancer. Currently, treatment options for endometriosis are limited to surgical removal of the endometrial lesions and symptomatic management. However, these treatments are associated with significant challenges, including limited efficacy, fertility concerns, and recurrent symptoms. Our goal is to identify and develop additional therapeutic targets and treatment options for endometriosis.

Method:
Given the prevalence of kinases as FDA-approved drugs, we performed an analysis of overexpressed kinases in endometriotic lesions compared to normal eutopic endometrial tissues (CE) and patient endometrium from a previously published dataset (GSE141549). We identified Ephrin receptor A2 (EPHA2) and Ephrin receptor A4 (EPHA4) kinases as potential non-hormonal therapeutic targets for endometriosis based on their significantly elevated expression levels in the endometriotic lesions compared to CE. To discover potent and selective small molecules that inhibit the kinase activity of EPHA2 and EPHA4, we screened around 5 billion compounds using a DNA-encoded chemistry technology (DEC-Tec) approach. Hit compound (CDD-2693) and optimized compound (CDD-3167) were tested for biological activity in 12Z, an endometriotic epithelial cell line and patient-derived organoids.

Result:
Hit compounds identified from DEC-Tec selection displayed a picomolar/nanomolar potency in inhibiting EPHA2/4 kinase domains using *in vitro* biochemical assay. Further optimized hit compounds, CDD-2693 and CDD-3167, demonstrated potent inhibition of ephrin-mediated activation of EPHA2/4 in 12Z cells. CDD-3167 is showing a significant inhibition effect starting at 1 nM concentration. To test the therapeutic potential of our inhibitors in the context of inflammation, given one of the hallmarks of endometriosis is to induce a pro-inflammatory state in the ectopic lesions, we examined the expression level of *PTGS2*, a pro-inflammatory gene, upon the treatment of our inhibitors during an IL-1β challenging assay in 12Z cells. Both CDD-2693 and CDD-3167 decreased the *PTGS2* expression in the presence of IL-1β, with an IC50 of 7.2 μM and 1.3 μM, respectively. We further validated the therapeutic effect of CDD-2693 and CDD-3167 in patient-derived endometrial organoids. Unlike the vehicle-treated organoids, which continued to expand in diameter over the course of the culturing, organoids treated with the CDD-2693 and CDD-3167, showed a significant decrease in diameters after 72 hours of treatment.

Conclusions:
We demonstrated ephrin receptor kinase family is an actionable drug target for endometriosis and we report the discovery of potent EPH kinase inhibitors using DEC-Tec screening of a multi-billion compound collection. Optimized hit compounds demonstrated excellent inhibition and showed exceptional cellular pan-EPH kinase selectivity. Additionally, we exemplify our initial use of these ephrin receptor kinase inhibitors for advancing the treatment options for of endometriosis.

– continued on page 15

– *continued from page 14*

Health and Human Development (R01HD105800, HD096057 (D.M.) and R01HD110038 (M.M.M.)). DM is supported by a Next Gen Pregnancy Award from the Burroughs Welcome Fund (NGP10125). C.J.C. is supported by the Dan L. Duncan Cancer Center Grant CA125123. M.P. is supported by NIH grant R03CA259664 and a grant from the Cancer Prevention Research Institute of Texas (RP220524).

ID# 5

Rituximab Induced Late Onset Neutropenia in a Patient with Myelin Oligodendrocyte Glycoprotein (MOG) Antibody Disease, Mimicking a Myeloid Malignancy

Chihoon Ahn[1], Sunil Patel[2], Mike Perez[1], Andreia N. Barbieri[1]

[1]Baylor College of Medicine, Department of Pathology and Immunology
[2]Kelsey-Seybold, Department of Hematology and Oncology

Introduction
Late onset neutropenia associated with rituximab has been reported in patients with autoimmune diseases or hematologic malignancies, with rare cases reported after rituximab treatment for neuroinflammatory disorders such as multiple sclerosis or myelin oligodendrocyte glycoprotein antibody-associated disease.

Case Presentation
We present a 31-year-old male patient with 10-year history of MOG antibody disease, treated with natalizumab for an unknown number of years, with subsequent rituximab every 6 months for 4 years prior to presentation at our institution. The patient presented with febrile neutropenia 3 months after the last dose of rituximab, without evidence of active infection.

Pathology
Peripheral blood smear and flow cytometry showed absolute neutropenia, with B cell depletion, and relative monocytosis. A bone marrow biopsy was performed, showing markedly left-shifted myeloid proliferation and maturation arrest, with numerous promyelocytes and myelocytes, although with mild hypocellularity for age. Blasts were not increased as evidenced by flow cytometry or CD34 immunohistochemical staining. Chromosome analysis revealed a normal male karyotype in all cells analyzed. The patient received intravenous antibiotics, rituximab was discontinued, and neutrophil counts began to recover following discharge from the hospital.

Conclusions
Awareness of potential changes in the peripheral blood and bone marrow in rare cases of rituximab-induced LON, with associated maturation arrest at the promyelocyte stage, is essential to assist pathologists in providing an accurate diagnosis in patients with MOG antibody disease or other neuroinflammatory disorders and neutropenia.

– continued on page 17

– *continued from page 16*

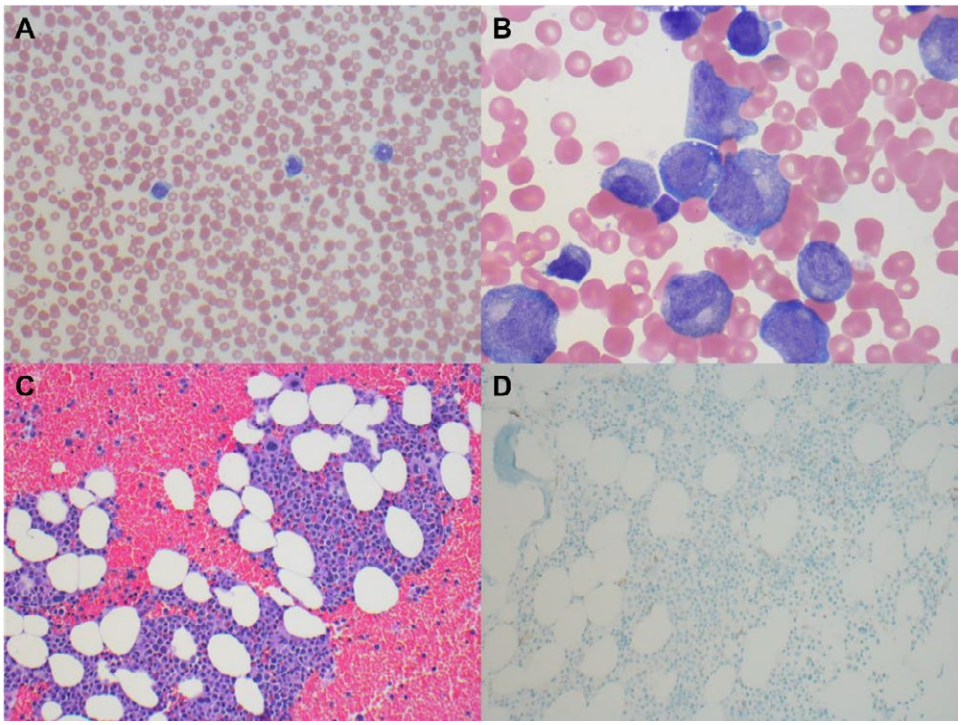

ID# 6

Late Relapse of a Testicular Teratomatous Mixed Germ Cell Tumor as an Invasive Adenocarcinoma, Somatic-Type Malignancy in Retroperitoneal Lymph Nodes – A Diagnostic Pitfall

Chihoon Ahn[1], Chris J. Finch[1, 2], Ya Xu[1, 2]

[1] Department of Pathology & Immunology, Baylor College of Medicine, Houston, TX

[2] Department of Pathology & Laboratory Medicine, Ben Taub General Hospital, Harris Health System, Houston, TX

Introduction
Somatic-type malignancies of testicular germ cell tumors are rare, and usually associated with teratomatous germ cell tumors. Carcinomas are less common than sarcomas and often appear late in the course of the disease. Here, we report a somatic-type malignancy in retroperitoneal lymph nodes, associated with testicular mixed germ cell tumor.

Case Presentation
The patient was a 31-year-old male with a past medical history of testicular mixed germ cell tumor (embryonal carcinoma 80%, yolk sac tumor 15%, and teratoma 5%) by orchiectomy, and retroperitoneal lymphadenopathy (3.5 cm) by computer tomography (CT) of abdomen and pelvis 7 years ago. He was lost to follow-up for half a year and then received three cycles of chemotherapy (cisplatin, etoposide and ifosfamide) for innumerable bilateral pulmonary metastasis and retroperitoneal lymph node conglomerate (10.6 cm) by imaging. Five years later, CT showed retroperitoneal conglomerate lymph nodes increased in size from 3.8 cm to 5.2 cm and developed mass effect to duodenum in four months. He underwent partial duodenectomy and dissection of retroperitoneal lymph nodes.

Pathology
Histologic examination of the specimen showed the serosa of duodenum and multiple lymph nodes involved by an adenocarcinoma. The tumor was arranged predominantly in glandular structures with mucinous features, resembling the teratoma component composed of columnar cells with supranuclear mucin in glands in the previous orchiectomy specimen. Immunohistochemical stains revealed the adenocarcinoma was positive for CDX2, CK20, and negative for CK7, CD30, SALL4, PLAP, while the teratoma component within the orchiectomy specimen was positive for CDX2, CK20, CK7 (patchy), SALL4, and negative for CD30 and PLAP. The diagnosis of a late relapse of a testicular teratomatous mixed germ cell tumor as an invasive adenocarcinoma, somatic-type malignancy in retroperitoneal lymph nodes was rendered.

Conclusion
Somatic-type malignancies associated teratoma usually occurs in retroperitoneal lymph nodes with poor prognosis, post cisplatin-based chemotherapy, as that seen in the current case. Our study demonstrates the pathological features of somatic-type malignancy associated with a testicular teratomatous mixed germ cell tumor as an invasive adenocarcinoma, which can be a diagnostic pitfall since the tumor mimics primary gastrointestinal malignancy histologically and immunohistochemically.

ID# 7

Rare Case of Basal Cell Carcinoma in an African American Child With Gorlin-goltz Syndrome

Mokhtar Abdelhammed[1], Sharon Plon[2], Jed Nuchtern[2], Nino Rainusso[2], Kalyani Patel[1]

[1]Pathology & Immunology, Baylor College of Medicine, TX

[2]Texas Children's Cancer Center, Baylor College of Medicine, TX

INTRODUCTION:

Nevoid basal cell carcinoma Syndrome NBCCS (also Gorlin-Goltz syndrome, GGS), is a rare autosomal dominant condition with the classic triad of basal cell carcinoma (BCC), keratocystic odontogenic tumor/s (KCOT) and skeletal malformations. Development of BCCs is typically in adolescence or early adulthood in this syndrome and more frequent in individuals of European ancestry. Acrochordon-like lesions is the most common clinical presentation and nodular, follicular or infundibulocystic are common histologic variants.

CASE PRESENTATION:

We present a 15-year-old African American girl with KCOTs, calcification of the tentorium, and a new development of an atypical nodulocystic lesion on the chest wall.

PATHOLOGY:

Beside the unique nodulocystic gross features, the chest wall lesion showed a rare adenoid cystic variant of BCC. Additionally, the patient had a mutation in PTCH1 c.2887+1G>A with a mosaic variant of NBCCS.

CONCLUSION:

This case is a rare presentation of a pediatric BCC in an African-American patient with a nodulocystic lesion and unusual adenoid cystic histologic features. This case also emphasizes the significance of a multi-disciplinary approach in managing these complex patients.

ID# 8

Pediatric Antibody-mediated Rejection in Pediatric Lung Transplantation: Unraveling Histopathological Insights

Authors: M. Abdelhammed, D. Leza-Rincon, D. Schady, S. Nicholas, D. Moreno-McNeil, E. Melicoff-Portillo, N. Cortes-Santiago

Baylor College of Medicine, Houston, Texas, US

INTRODUCTION:

Diagnosing antibody-mediated rejection (AMR) post-lung transplantation remains an intricate and complex task. We aim to delineate the histopathological findings within a group of pediatric lung transplant recipients who were diagnosed with, and treated for AMR at a large pediatric institution.

METHODS:

Institutional database was searched to identify pediatric lung transplant patients who underwent treatment for AMR between 2017-2022. Relevant demographic, clinical, and laboratory data were obtained from the electronic medical records. Diagnostic and follow up biopsy slides, including C4d immunohistochemistry were reviewed. Acute cellular rejection was graded according to ISHLT criteria. The presence of eosinophils was categorized as absent (0), rare (1), or greater than rare (2). A score higher than rare was assigned if there was at least 1 eosinophil in three or more high-power fields (hpf) or if eosinophil microabscess-like clusters were observed, even if only focally. Neutrophils were graded as absent (0), less than 10/hpf (1), 10-20/hpf (2), and more than 20/hpf (3). Distribution and strength of C4d was graded as focal/diffuse and weak/strong, respectively.

RESULTS:

Nine patients met inclusion criteria. The indications for transplantation were varied and included cystic fibrosis (2), pulmonary veno-occlusive disease (2) and ABCA3 surfactant deficiency (2), among others. The median age at transplantation was 34 months (3-191 months), and median post-transplant interval at AMR was 1 month (0.2-53 months). Seven patients developed AMR within 3 months of transplant. Diagnostic biopsy findings included tissue eosinophils (any) in 5 cases, acute lung injury in 4, and septal neutrophilia (2+) in 3. Diffuse and strong C4d was seen in 5 patients. Two biopsies showed significant concomitant acute cellular rejection (>A2). Lymphocytic bronchiolitis was seen in 4. Four patients had died at the conclusion of this study, at a median post-AMR diagnosis of 1.5 months (range: 1-20 months). Three deceased patients had evidence of persistent acute lung injury with death occurring less than 3 months after AMR diagnosis.

CONCLUSION:

AMR frequently occurs in the early post-transplant period in the pediatric lung transplant population. Acute lung injury is an important injury pattern in pediatric AMR and portends an unfavorable prognosis.

ID# 9

AI-All Inclusive- Artificial Intelligence Cannot Outsmart the Clinical Chemist

Ridwan B Ibrahim[1, 2], Anil K Chokkalla[1, 2], Sneha Kumar[1] and Sridevi Devaraj[1, 2]

[1]Department of Pathology & Immunology; Baylor College of Medicine; [2]Department of Pathology, Texas Children's Hospital, Houston, Tx, USA.

ABSTRACT:

Introduction: The rise of Artificial intelligence (AI) tools and their use has gained popularity among people from different works of life. Their ability to generate human-like answers in a conversational context sparked a massive interest in people with calls for its application in different areas like healthcare etc. We evaluated the utility of artificial intelligence–powered language models (Google Bard, ChatGPT 3.5 and GPT-4) compared to trainees and clinical chemists in responding to common laboratory questions in the broad area of Clinical Chemistry.

Methods: 35 questions from clinical consultations, real-life case scenarios, and clinical chemistry questions were used to evaluate these AI tools alongside clinical chemistry trainees and clinical chemistry faculties. Responses were scored by a blind participant and scores assigned and calculated in percentages as either being correct, partially correct or incorrect. Additionally, responses were ranked based on categories and years of experience.

Results: Of the 35 questions asked, all human participants performed better than the AI tools. The Senior Chemistry Faculty demonstrated superior accuracy with 100% of correct responses compared to 71.4, 82.9% and 90.5% of correct responses from the residents, fellows and junior chemistry faculty. Both Google Bard and ChatGPT 3.5 generated 60% correct responses while GPT-4 generated 71.4% correct responses respectively. Of the sub-categories examined, both Google Bard and GPT-4 did not achieve 100% accuracy in any subcategory while ChatGPT 3.5 achieved 100% accuracy in endocrinology. GPT-4 performed better than both Google Bard and ChatGPT 3.5 but performed poorly to human participants when both partially correct and incorrect indices were considered.

Conclusions: We evaluated the performance of the popular AI-tools in answering questions in the field of clinical chemistry compared to responses given by individuals specially trained in the field of clinical laboratory medicine. Despite advances in AI-powered language models, Google Bard, ChatGPT 3.5 and GPT-4 cannot replace a trained pathologist in answering clinical chemistry questions. Caution should be observed by people, especially those not trained in clinical chemistry, to interpret test results using these tools.

ID# 10

Delayed Histiocytic Foreign Body Reaction and Granuloma Formation After Argiform Injection for Soft Tissue Augmentation: A Case Report and Review of the Literature

Mokhtar Abdelhammed[1], Lois M. Dodson[1], *Abdul H. Diwan[1],* Ya Xu[1, 2]

[1] Department of Pathology & Immunology, Baylor College of Medicine, Houston, TX

[2] Department of Pathology & Laboratory Medicine, Ben Taub General Hospital, Harris Health System, Houston, TX

INTRODUCTION:
With cosmetic procedures being in popular demand and the growing fever for rejuvenation, the epidemic usage of non-approved tissue expanders by unlicensed or trained practitioners in nonmedical settings is constantly on the rise. Several tissue augmenting agents have been developed with different biodegradable properties and indications approved by the US-FDA body. We report histiocytic foreign body reaction and granuloma formation after Argiform injection for buttock augmentation.

CASE PRESENTATION:

A 31-year-old female with unremarkable past medical history who presented with 2-year-old bilateral rashes on her buttocks. Initially, it was confined to her right buttock then extended to the left side after several months and was associated with scaps, Itchiness and pain. On examination, a 4.0 cm plaque in its greatest dimension was noted. Despite triamcinolone and hydrocortisone topical ointments, her symptoms persisted. Refractory to treatment and unclear history, a punch biopsy was recommended.

PATHOLOGY:
Histopathological findings concluded histiocytic reaction to foreign material resembling lipoblast-like cells prompting additional history inquiries. Consequently, the patient reported that she had received cosmetic Argiform injections at a local Spa center 4-5 years prior to her presentation. Several treatment options are proposed with variable success rates depending on the nature of the cosmetic agent. Resorbable fillers are readily degraded via the host and the first choice of treatment of foreign body granulomas caused by them are either systematic or intralesional corticosteroid injections. However, since our patient was injected with Argiform, a permanent non-biodegradable filler, its secondary granulomas are generally considered more challenging to address and surgical intervention is the mainstay.

CONCLUSION:

Histopathological examination remains the gold standard modality to identify the responsible filler agent. As a result, it is of utmost significance that both dermatopathologist and dermatologist be familiar with the spectrum of microscopic findings that is unique for each individual tissue expander, be aware of rare forms of tissue augmenters along with obtaining thorough history for more accurate recognition and ultimately proper management.

ID# 11

Comparison of Cervical Pap Smears with Positive High-risk Human Papillomavirus (hrHPV) Tests with Non-HPV 16/18/45 HPV Subtypes and HPV 16/18/45 Subtypes Including Cyto-histologic Correlation

Authors: Jennifer Addo, MD, Cameron Brown, PhD, Ya Xu, MD, PhD,
Department of Pathology and Immunology, Baylor College of Medicine, Houston, TX
Department of Pathology and Laboratory Medicine, Ben Taub Hospital, Harris Health System, Houston, TX

Background:
The analysis of the cervical Pap smears with positive hrHPV tests with non-HPV 16/18/45 subtypes is very limited. We aim to provide data on the Pap smears with non-HPV 16/18/45 subtypes compared to those with HPV 16/18/45 subtypes.

Design:
We collected Pap smears (ThinPrep) with positive hrHPV tests from 2019 to 2023 in our institution. Cases with non-HPV 16/18/45 subtypes (group A), and with HPV 16/18/45 subtypes (group B) were evaluated for the diagnostic categories and odds ratios (OR). Cyto-histologic correlation on the category of high-grade squamous intraepithelial lesion (HSIL) was conducted.

Results:
We reviewed a total of 5263 cases of Pap smears with positive hrHPV tests. Among these 5263 cases, group A (non-HPV 16/18/45 subtypes) contained 4224 cases (80.3%, 4224/5263), and group B (HPV 16/18/45 subtypes) had 1039 cases (19.7%, 1039/5263). *The main diagnostic categories were:* unsatisfactory for evaluation/non-diagnostic, 42 cases (0.99%, 42/4224) in group A and 8 cases (0.77%, 8/1039) in group B; negative for intraepithelial lesion or malignancy (NILM), 1416 cases (33%, 1416/4224) in group A and 168 cases (16%, 168/1039) in group B; atypical squamous cells of undetermined significance (ASC-US), 1184 cases (28%, 1184/4224) in group A and 269 cases (25.9%, 269/1039) in group B; low-grade squamous intraepithelial lesion (LSIL), 1368 cases (32%, 1368/4224) in group A and 416 cases (40%, 416/1039) in group B; atypical squamous cells, cannot exclude HSIL (ASC-H), 91 cases (2.2%, 91/4224) in group A and 52 cases (5%, 5/1039) in group B; HSIL, 81 cases (1.9%, 81/4224) in group A and 102 cases (9.8%, 102/1039) in group B. Group A had higher odds ratios (OR) for NILM (2.59), and lower OR for LSIL (0.71), ASC-H (0.42), and HSIL (0.18). The cyto-histologic correlation on the category of HSIL displayed the histologic diagnosis of at least HSIL in 87.5% of follow-up cervical biopsies in group A and 96.8% in group B.

Conclusion:
Pap smears positive for hrHPV tests have a high proportion of non-HPV 16/18/45 subtypes (80.3%) in our patient population, which is predominantly Hispanic/Latina and non-Hispanic black. Cyto-histologic correlation of HSIL shows higher consistency in the group with HPV 16/18/45 subtypes. The group with non-HPV 16/18/45 subtypes were more likely to be NILM on cytology (OR: 2.59), indicating that co-testing with significant importance in such a population, as Pap smear alone may miss detecting patients with hrHPV, non-HPV 16/18/45 subtypes.

ID# 12

Large Atypical Lipomatous Tumor/Well-Differentiated Liposarcoma of Buccal Mucosa: Report of a Rare Case

Lucas A. McGowan, MD[1], Zipei Feng, MD[2], David J. Hernandez, MD[2, 3], Ya Xu, MD, PhD[1,4]

[1]Department of Pathology & Immunology, Baylor College of Medicine, Houston, TX

[2]Department of Otolaryngology – Head & Neck Surgery, Baylor College of Medicine, Houston, TX

[3]Department of Otolaryngology, Ben Taub Hospital, Harris Health System, Houston TX

[4]Department of Pathology, Ben Taub Hospital, Harris Health System, Houston TX

Introduction

Liposarcoma is not common in the head and neck, and extremely rare in the oral cavity: 7% occur in the head and neck and 0.3% in the oral cavity. We report an atypical lipomatous tumor/well-differentiated liposarcoma (ATL/WDL) of buccal mucosa with recurrence.

Case Presentation

A 66-year-old female presented with a right facial mass that had been present for over 10 years and resected 6 times as lipoma in her home country. The mass had grown since the last resection two years ago. Computerized tomography of neck soft tissue displayed a heterogeneous 11 cm mass with fat density in the right buccal mucosal spaces, and a 4.8 cm connecting solid nodule in the right pharyngeal mucosal space. Complete resection of the mass/nodule was performed.

Pathology

Grossly, the specimen consisted of two nodular masses (separately cut during operation), 13.1 cm and 7 cm, respectively. The cut surfaces of the masses revealed yellow fatty tissue with focal fleshy areas corresponding to the nodule with solid density by imagining. Microscopically, the squamous mucosa had a lipomatous tumor composed of sheets of well-differentiated adipocytes that infiltrated the underlying and surrounding skeletal muscle and connective tissue. Upon extensive sampling, scattered lipoblasts were found in relatively cellular areas. The nonlipogenic stromal cells with nuclear pleomorphism were seen in the fibrous/solid areas. No mitosis or necrosis was identified. MDM2 amplification was detected by fluorescent in situ hybridization (FISH). These findings support the diagnosis of recurrent ATL/WDL.

Conclusions

We demonstrate the histological features of a large atypical lipomatous tumor/well-differentiated liposarcoma of buccal mucosa. Extensive sampling of the specimen to identify the lipoblasts and atypical stromal cells, and MDM2 FISH study on suspicious cases are the keys to achieve accurate diagnosis. The high recurrence rate of this entity in the head & neck region exhibited in this case warrants the need of long-term follow-up.

– continued on page 25

– *continued from page 24*

Liposarcomas are extremely rare in the oral cavity and can be a challenging diagnosis to make. This patient's previous resections were misdiagnosed as lipoma in her home country. Recurrence of this locally aggressive tumor can occur more frequently without proper treatment due to incorrect diagnosis, as shown in this case report.

ID# 13

Senile Seminal Vesicle Amyloidosis in a Radical Prostatectomy Specimen

Katelyn Moss, DO[1], Bettye Cox, MD[1, 2], Ya Xu, MD, PhD[1, 3]

[1] Department of Pathology & Immunology, Baylor College of Medicine, Houston, TX

[2] Department of Pathology, Baylor St. Luke's Medical Center, Houston, TX

[3] Department of Pathology & Lab Medicine, Ben Taub Hospital, Harris Health System, Houston, TX

Introduction

Localized and isolated amyloid deposits can be seen in various organs including those in the genitourinary tract. Amyloidosis within the seminal vesicles, ejaculatory ducts, and vas deferens is uncommon and usually found incidentally in surgical specimens and considered to be related to aging. Here we report a case of amyloidosis in seminal vesicles with typing of the amyloid peptide profile.

Case Presentation

The patient was a 65-year-old man with a past medical history of diabetes mellitus, hypertension, elevated prostate-specific antigen (PSA, 4.5 ng/ml), biopsy-confirmed prostate cancer, and no evidence of metastatic disease by imaging. The patient underwent a radical prostatectomy three months after the prostate biopsy.

Pathology

Grossly, the radical prostatectomy specimen consisted of a prostate (35.7grams and 4 cm), and bilateral seminal vesicles (3.3 cm and 2.2 cm, respectively). Microscopically, there was prostatic adenocarcinoma (Gleason score 4+5). The bilateral seminal vesicles had no tumor involvement, but showed diffuse subepithelial eosinophilic and amorphous proteinaceous material deposition. The proteinaceous material was highlighted by Congo red special stain and showed apple-green birefringence under polarized light. Liquid chromatography tandem mass spectrometry (LC MS/MS) was performed in a reference lab and detected a peptide profile consistent with Asem 1 (semenogelin 1)-type amyloid deposition. The additional diagnosis of senile seminal vesicle amyloidosis (SSVA) was rendered.

Conclusions

Senile seminal vesicle amyloidosis (SSVA) is a type of organ-limited amyloidosis with unique histological features and protein profiles. Its approximate incidence is approximately 4.7% of radical prostatectomy specimens by studies. The amyloid deposits are incidentally found in the subepithelial region of the entire seminal tract including seminal vesicles, ejaculatory ducts, and vas deferens, as well as isolated involvement of one portion. These amyloid deposits are the result of accumulation of one of the secretory products of the seminal vesicle, Semenogelin 1 and are permanganate sensitive. SSVA can be misinterpreted on magnetic resonance imaging (MRI) as tumor involvement by prostatic or urinary bladder carcinoma. Awareness of this entity and careful examination of the seminal tract of the surgical specimens are important.

ID# 14

Choroid Plexus Carcinoma and its Association with Li-Fraumeni Syndrome

Katelyn Moss, DO; John Van Arnam, MD; Melissa Blessing, DO

Baylor College of Medicine / Texas Children's Hospital, Houston, TX USA

Introduction

Choroid plexus carcinoma (CPC) is a rare neoplasm of the specialized epithelium that produces cerebrospinal fluid (CSF). The majority of cases occur in infants and young children and present with variable symptoms, sometimes acutely, associated with hydrocephalus. Genetic susceptibility for this neoplasm is associated with Li-Fraumeni syndrome.

Case Presentation

We present a case of a 2 year old male, previously well, who presented with a one month history of progressive nausea, vomiting, and lethargy. His symptoms were nonresponsive to famotidine and lansoprazole. Ultimately, he presented comatose to the emergency department, where a head CT noted a 7.2 x 6.0 x 4.5 cm right posterior temporal mass with cystic/necrotic changes and herniation. During transfer for a higher level of care he developed pulseless arrest and died. A limited brain and spinal cord only autopsy was performed.

Pathology

At autopsy, the brain showed a 6.7 x 6.5 x 4.2 cm tan-grey papillary mass circumferentially coating and markedly expanding the temporal and occipital aspects of the right lateral ventricle with associated severe cerebral edema and mass effect resulting in midline shift and herniation. Microscopic examination demonstrated a papillary to solid neoplasm invading brain parenchyma with broadly pushing borders, variably hyperchromatic nuclei, irregular nuclear contours, brisk mitotic activity and corresponding high Ki67 labeling, and necrosis. Immunostains confirmed the choroid plexus origin of the tumor and p53 showed a wild-type pattern.

Conclusions

In this case, the family's main question was about the genetic associations with this tumor and whether their future children were at risk of similar tumors. Pediatric autopsy is an important and valuable tool for pathologists to aid families in understanding genetic implications of a child's death as well as future family planning. Li-Fraumeni syndrome is an autosomal dominantly inherited germline mutation in the TP53 gene which results in increased risk of developing various cancers. Most patients with this syndrome inherit an altered copy of the gene from an affected parent, but 7-20% of cases are the result of a de novo mutation. A limited genetic study of the patient and parents in this case yielded important information about their own risk as well as their future offspring's risk of having this genetic syndrome and developing cancer.

ID# 15

NEDDylation is Essential in Pathways Dysregulated with Oocyte Aging

Avery A. Ahmed[1,2], Bethany K. Patton[3], Peixin Jiang[1], Matthew Meyer[4], Stephanie A. Pangas[1,2,3,5,6]

[1]Department of Pathology & Immunology, Baylor College of Medicine, Houston, TX, USA.
[2]Graduate Program in Development, Disease Models & Therapeutics, Baylor College of Medicine.
[3]Graduate Program in Molecular & Cellular Biology, Baylor College of Medicine.
[4]Shared Equipment Authority, Rice University, Houston, Texas, USA.
[5]Graduate Program in Biochemistry & Molecular Biology, Baylor College of Medicine.
[6]Department of Molecular & Cellular Biology, Baylor College of Medicine.

Introduction

Oocytes are unique cells that face the difficult task of maintaining quality during decades of quiescence to produce healthy offspring. Oocyte quality decline over time is an established phenomenon that leads to increasing infertility rates in women over 35. Specifically, key processes such as chromatin organization and mitochondrial function significantly decline over time. As the average age of childbearing continues to increase worldwide, understanding mechanisms that underlie this decline will assist in maintaining women's reproductive health. Our goal is to determine pathways involved in oocyte quality control, including posttranslational modifications (PTMs) such as NEDDylation.

Methods

Using CRISPR/Cas9 gene editing, we generated a novel conditional allele of *Uba3*, an essential enzyme in the NEDDylation pathway, and crossed it with the oocyte-specific cre driver line, *Gdf9-icre* to produce the first oocyte-specific knockout of NEDDylation ("*Uba3* cKO"). To investigate reproductive disease and infertility, we performed fertility studies, analyzed ovulation by exogenous hormonal stimulation, measured circulating serum hormone levels, and quantified the number of follicles of different developmental stages from 3 week, 6 week, 8 week, and 12 week-old-mice. We utilized immunofluorescent staining to visualize protein abundance and chromatin state in isolated oocytes. We further analyzed *Uba3* cKO oocytes for mitochondrial dysfunction using Seahorse assays and transmission electron microscopy.

– continued on page 29

– *continued from page 28*

Results

In a six-month fertility trial with continuous mating of control and *Uba3* cKO females to wild-type males, *Uba3* cKO mice failed to produce any pups. *Uba3* cKO ovaries showed a significantly reduced number of follicles of every developmental stage compared to controls beginning at 8 weeks of age; by 12 weeks of age, follicles were nearly depleted. At 8 weeks of age, serum levels of anti-Mullerian hormone (AMH) were significantly decreased in *Uba3* cKO and by 6 months this decrease was more pronounced. Six-month-old *Uba3* cKO mice also showed significant dysregulation of circulating sex hormones: luteinizing hormone (LH) and follicle-stimulating hormone (FSH). When exogenously stimulated, *Uba3* cKO mice ovulated significantly fewer oocytes than controls and, of those that were ovulated, a significantly higher proportion were dead. *Uba3* cKO oocytes were unable to condense chromatin as indicated by the lack of transition from non-surrounded nucleolus (NSN) to surrounded nucleolus (SN) at the fully grown oocyte stage. Functionally, *Uba3* cKO oocytes exhibited significantly decreased maximal and basal respiration rates. On a subcellular level, oocyte mitochondria showed increased occurrence of vacuolization, a detrimental apoptotic mitochondrial phenotype, in *Uba3* cKO mice compared to controls.

Conclusions

Uba3 cKO oocytes exhibit characteristics clinically associated with human oocyte quality decline with aging: lower ovarian reserve, mitochondrial dysfunction, and chromatin state disruption. These combine to render *Uba3* cKO mice sterile. This work identifies NEDDylation as a crucial regulatory component of oocyte quality, and determining specific NEDD targets could contribute to the diagnostic repertoire of what makes a ‘good’ oocyte.

ID# 17

Capecitabine-induced Colitis: A Rare Potentially Fatal Adverse Event

Sonal L Italiya M.D[1], Nisha Ramani M.D[1,2], Linda K Green M.D[1,2]
[1]Department of Pathology & Immunology, Baylor College of Medicine, Houston, TX
[2]Michael E. DeBakey VA Medical Center, Houston, TX

Introduction: Capecitabine is an oral 5-fluorouracil prodrug and is commonly used in the treatment of advanced colorectal, gastric, biliary tract, and breast carcinoma. Capecitabine use-associated gastrointestinal side effects are common but can be managed effectively. Capecitabine-induced enteritis and colitis are rare and under-reported even though it has the potential for severe adverse events and require permanent therapy withdrawal.

Case presentation: A 50-year-old male came to the hospital with watery diarrhea and severe abdominal pain. He was prescribed oral capecitabine chemotherapy for his recently diagnosed rectal adenocarcinoma. Abdominal CT scan and colonoscopy revealed diffuse colonic thickening, edema, and visible erythema throughout the colon. Endoscopic biopsies were performed from multiple sites from the colon to the rectum.

Pathologic and ancillary findings: The biopsies from the colon and rectum showed severe acute ulceration, distorted crypt architecture, mixed inflammatory infiltrate in lamina propria, focal crypt abscesses, eosinophils and "squamoid-like" reparative atypia mimicking dysplasia. The features appeared to mimic ulcerative colitis but the "squamoid atypia" was unusual. True pseudomembranes were not seen. Immunohistochemistry for CMV and HSV were negative. We diagnosed this case as capecitabine-induced colitis and the clinical history was correlated which showed that the patient was taking double his recommended dose of capecitabine.

Discussion and Conclusion: Histological description for capecitabine-associated colitis is difficult to find in the published literature because the findings are similar to other causes of severe colitis. The clinical history is very important in recognizing this cause of colitis as it is directly dose-related. After discontinuation of capecitabine, our patient's abdominal pain quickly resolved, and his overall condition improved after further conservative management. Capecitabine is a widely used chemotherapeutic agent and the pathologist needs to be aware of its toxic effect on the gastrointestinal tract. We have also detected these strange "squamoid-like" cytopathic changes in other resected colorectal cases who previously received capecitabine. This may be a helpful histologic finding to suggest capecitabine-associated colitis. We are certain that the recognition of this entity allowed for a rapid recovery in our patients.

ID# 17

A Study of the Cause of Death in Stillbirths in a Tertiary Medical Center

Authors:

Elizabeth M Taylor[1], Briana Fernandez[1], Ya Xu[1]

[1] Baylor College of Medicine

Background:

The stillbirth rate in the United States is higher than that of many other developed countries. The causes of a great number of stillbirths remain unexplained. This study is to analyze the cause of death of the stillbirths in our patient population, predominantly Black and Hispanic or Latina.

Methods:

We searched the database in our hospital, a tertiary medical center, and selected completed autopsy cases of stillbirths in the years of 2012 – 2023. The causes of death of stillbirths were analyzed by review of the postmortem examination, placental pathology, and medical record. A potential cause of fetal death was graded as being a probable cause of death, a possible cause of death, or a present condition, which was developed by the Stillbirth Collaborative Research Network investigators.

Results:

A total of 101 stillbirths consisting of 54 male fetuses (53%) and 47 female fetuses (47%) were reviewed. The maternal age at delivery ranged from 18 to 42 years old. The gestational ages were in the 3rd trimester with 54 cases (54%, 54/101) and the 2nd trimester with 47 cases (46%, 47/101). There were 97 cases (96%, 97/101) with placentas, and 4 cases (4%, 4/101) without placentas. The probable, possible, and present condition and/or undetermined causes of death were found in 63 cases (62%, 63/101), 22 cases (22%, 22/101), and 16 cases (16%, 16/101), respectively. The causes of death were placental abnormalities in 31 cases (31%, 31/101), infections in 21 cases (21%, 21/101) including fetal infection (2 cases), placental infection (16 cases) and both (3 cases), fetal structural/genetic abnormalities in 11 cases (11%, 11/101), obstetric complications in 8 cases (8%, 8/101), maternal medical conditions in 8 cases (8%, 8/101), umbilical cord abnormalities in 4 cases (4%, 4/101), other conditions such as hydrops fetalis in 2 cases (2%, 2/101), and undetermined causes in 16 cases (16%, 16/101). The causes of death related to placenta involved in 50 cases (50%, 50/101), including placental abnormalities and placental infections.

Conclusion:

– continued on page 32

– *continued from page 31*

Our data demonstrated the most common causes of death in stillbirths were placental abnormalities, and infections including fetal infection, placental infection and both. There were 16% of the stillbirths with no clear causes of death. Placental examination displayed significant importance in stillbirth autopsies as placenta related causes of death involved half of the cases studied in our patient population, predominantly Black and Hispanic or Latina.

ID# 20

Title: Congenital Pulmonary Airway Malformation Type 1 with Pulmonary Neuroendocrine Cell Hyperplasia in an Adult Male a Rare Case Report

Authors and Affiliations: Georgia Huffman[1], MD, Ya Xu, MD, PhD[1,2]

[1]Department of Pathology & Immunology, Baylor College of Medicine, Houston, TX

[2]Department of Pathology and Laboratory Medicine, Ben Taub Hospital, Harris Health System, Houston, TX

Introduction: Congenital pulmonary airway malformations (CPAM) is rare, usually diagnosed in the pediatric population, and may occur in adults. Pulmonary neuroendocrine cell hyperplasia (PNECH) mimicking diffuse idiopathic pulmonary neuroendocrine cell hyperplasia (DIPNECH) associated with CPAM has not been described previously. We report a case of CPAM Type 1 with PNECH.

Case Presentation: A 33-year-old male, with past medical history of latent tuberculosis (TB) by Quantiferon blood testing, recurrent pneumonia, recurrent lung abscesses, and lung cavitary lesion for three years, presented with fever, cough with hemoptysis, shortness of breath, and left-sided chest pain. Computerized tomography (CT) of chest displayed a 10.5 cm cavitary lesion in the left lower lobe of the lung. The patient underwent left lower lobectomy of the lung.

Pathology: Grossly, the lobectomy specimen revealed a 10.5 cm irregular cavity communicating to the superior segmental bronchus of the left lower lobe. Microscopically, the dominant large cyst was surrounded by lung parenchyma and small cystically dilated spaces resembling bronchioles under the fibrotic pleura. The large cyst was lined by respiratory epithelium with rare pathognomonic mucous cells in clusters. Cyst walls contained smooth muscle, small islands of cartilage, and focal intense acute and chronic inflammatory cell infiltrates with hemorrhage. There were multiple foci of proliferation of pulmonary neuroendocrine cells centered around bronchioles surrounding the large cyst.

– continued on page 34

– *continued from page 33*

Conclusions:

In this study, we reported the histologic features of a rare case of clinically and radiologically unrecognized congenital pulmonary airway malformations (CPAM) type 1 in a male adult. Additionally, pulmonary neuroendocrine cell hyperplasia (PNECH) was found associated with the CPAM, which has not been described previously. The PNECH mimics diffuse idiopathic pulmonary neuroendocrine cell hyperplasia (DIPNECH). The present PNECH may have been induced by underlying pulmonary inflammation/infection or may be idiopathic, and it is considered a pre-malignant condition.

Our study demonstrates a histologically diagnosed adult congenital pulmonary airway malformations type 1 with an incidental pulmonary neuroendocrine cell hyperplasia, which mimics diffuse idiopathic pulmonary neuroendocrine cell hyperplasia. To the best of our knowledge, this is the first report of such an association.

ID# 21

Microscopic Analysis of Human Endometrial Organoid Formation to Characterize the Endometrial Stem Cell Niche

Anna Catherine Unser[a,b], Suni Tang[a,b], Ting Geng[a,b], Linda Alpuing Radilla[c], Xiaoming Guan[c], Diana Monsivais[a]

[a]Department of Pathology & Immunology, Baylor College of Medicine, Houston, TX, 77030, USA
[b]Center for Drug Discovery, Baylor College of Medicine, Houston, TX, 77030, USA
[c]Department of Obstetrics and Gynecology, Baylor College of Medicine, Houston, TX, 77030, USA

Introduction: Endometrial organoids are an emerging 3D cell culture model to study reproductive disease and better understand the endometrial environment and tissue signaling *in vitro*. Within the endometrial environment, stem/progenitor cells capable of rapid regeneration are the cause of impressive tissue healing seen during a woman's menstrual cycle. Yet, the endometrial stem cell niche is not widely characterized. Our previous studies showed that genetic or pharmacological inhibition of the transforming growth factor-β (TGFβ) pathway activated the expression of the retinoic acid signaling pathway, including the expression of the aldehyde dehydrogenase (ALDH) enzymes, *Aldh1a1* and *Aldh1a3*. ALDH isoforms have previously been shown to lead to stem cell expansion in other organs.

Methods: To characterize the potential of ALDH as an endometrial stem cell marker, primary derived endometrial organoids from eutopic endometrium were subjected to fluorescence-activated cell sorting (FACS) using the ALDEFLUOR assay to select for $ALDH^{Hi}$ and $ALDH^{Lo}$ cells. We found that endometrial organoids from eutopic endometrium contained between 7.8%-18.1% $ALDH^{Hi}$ cells (n=5 donors), suggesting that a population of $ALDH^{Hi}$ cells is maintained in 3D organoid cultures. Endometrial organoids were then formed from the sorted ALDH cells and characterized according to growth potential using organoid formation assays. We also examined the effect of the TGFβ inhibitor, A83-01, which is an inhibitor of the ALK4/5/7 TGFβ type 1 receptors and used as a supplement in organoid media. For microscopic analysis, an inverted Zeiss Axioscope Phase Contrast Microscope was used to image and analyze organoid formation over 11 days.

Results: Organoid formation was analyzed using count and diameter of organoids of one representative image from each of three different wells using the Zeiss microscope over the course of 11 days. $ALDH^{Hi}$ and $ALDH^{Lo}$ organoids were then enzymatically dissociated into single cells, plated into a 3D matrix, and monitored over the course of 11 days. We found that compared to $ALDH^{Lo}$ organoids with A83-01 (9 ± 3 organoids) and without A83-01 (8 ± 3 organoids), $ALDH^{Hi}$ organoids had more organoids when grown in the presence of A83-01 (22 ± 7 organoids), but not in the absence (6 ± 2 organoids) of A83-01. We also observed that the diameters of $ALDH^{Lo}$ were smaller in the presence ($91\ \mu m \pm 25\ \mu m$) and absence of A83-01 ($20\ \mu m \pm 2\ \mu m$) compared to the diameters of $ALDH^{Hi}$ organoids cultured in the presence ($165\ \mu m \pm 22\ \mu m$) and absence ($84\ \mu m \pm 29\ \mu m$) of A83-01.

Conclusions: Overall, these results demonstrate that $ALDH^{Hi}$ organoids have a higher proliferative capacity in the presence of A83-01 and form more organoids with larger diameters compared to $ALDH^{Lo}$ organoids. These findings support the hypothesis that ALDH isoforms are enriched in stem cells of the endometrium.

Studies were supported by Eunice Kennedy Shriver National Institute of Child Health and Human Development (R01-HD105800) and the Burroughs Wellcome Fund Next Gen Pregnancy Award (NGP10125).

ID# 22

Integrated Analysis of the Human Fecal Microbiome and Metabolome Reveals the Therapeutic Role of Gut Microbiota Derived Indole-Derivatives in Endometriosis

Chandni Talwar[1], Goutham Venkata Naga Davuluri[1], Abu Hena Mostafa Kamal[2], Cristian Coarfa[2,3,4,5], Sang Jun Han[4], Surabi Veeraragavan[6], Krishna Parsawar[7], Nagireddy Putluri[2,4], Kristi Hoffman[8], Patricia Jimenez[9], Scott Biest[9,10], and Ramakrishna Kommagani[1,5,8,11*]

[1]Department of Pathology and Immunology, Baylor College of Medicine, Houston, TX, USA.
[2]Advanced Technology Cores, Baylor College of Medicine, Houston, TX, USA.
[3]Center for Precision and Environmental Health, Baylor College of Medicine, Houston, TX, USA.
[4]Department of Molecular and Cellular Biology Department, Baylor College of Medicine, Houston, TX, USA.
[5]Dan L Duncan Comprehensive Cancer Center, Baylor College of Medicine, Houston, TX, USA.
[6]Department of Molecular Human Genetics, Baylor College of Medicine, Houston, TX, USA.
[7]Analytical and Biological Mass Spectrometry Core Facility, University of Arizona, Tucson, AZ, USA.
[8]Alkek Center for Metagenomics and Microbiome Research, Baylor College of Medicine, Houston, TX, USA.
[9]Division of Reproductive Endocrinology and Infertility, Department of Obstetrics and Gynecology, Washington University School of Medicine, St Louis, MO, USA.
[10]Division of Minimally Invasive Gynecologic Surgery, Washington University School of Medicine, St Louis, MO, USA.
[11]Department of Molecular Virology and Microbiology, Baylor College of Medicine, Houston, TX, USA.

Correspondence to: Rama.Kommagani@bcm.edu

Introduction: Endometriosis is a chronic gynecological condition of high incidence in premenopausal women that is characterized by the benign endometrial proliferations at extrauterine sites. The condition primarily arises from retrograde menstruation that implants the endometrial tissue at ectopic sites. However, the resulting inflammation plays a key role in its pathogenesis as the disease progresses through macrophage infiltration and increased pro-inflammatory cytokines secretion in the peritoneal space. The disease is a serious burden with no identified cure, as the growing endometriotic lesions inflict pain and cause more serious reproductive health complications, such as infertility. In recent efforts to understand its pathogenesis, the gut microbiota has emerged as a key determinant of disease progression as it substantially impacts the peritoneal immunological milieu. However, the profiles of microbiota derived metabolites that provide a direct functional readout of the gut microbiome in endometriosis remain an unaddressed gap.

Methods: We utilized the advanced untargeted metabolomics approach to study the global profiles of the gut derived metabolites using the stool samples from women with and without endometriosis. For studying the gut microbiota profiles, we utilized the 16S rRNA gene

–continued on page 37

– *continued from page 36*

sequencing approach. Subsequently, we performed integrated analysis combing the microbiota and metabolomic profiles to identify correlation and the metabolites derived from gut microbiota.

Results: We identified a distinctive bacteria-derived metabolite signature intricately linked to endometriosis. Of clinical relevance, we found several metabolite markers of the disease which could pave the way for stool-based non-invasive diagnostic testing. Importantly, we found two gut bacteria-derived indole-derivates that are lower in stool samples of endometriosis. Both the metabolites reduced the in vitro cell viability of immortalized human endometriotic epithelial cells derived from human endometriotic lesions. Using extensive *in vivo* studies in both murine and humanized models of the disease, we found that these indole derived metabolites inhibited both the formation and progression of endometriotic lesions. The lesions derived from treated mice lacked characteristics typical of the progressing lesions such as proliferative epithelium, well-formed stroma and endometrial glands. Further, we found that the inflammation and macrophage infiltration was reduced in the peritoneal space upon treatment with these metabolites.

Conclusion: Gut microbiota derived metabolites of indole exhibit inhibitory effect on endometriosis disease progression. These findings open promising avenues for microbiota-based therapeutic interventions critical for the management of endometriosis.

ID# 23

SF3B1 Splicing Factor: A Key Player in Endometrial Cancer Tumorigenesis

Goutham. Davuluri[1], Pooja Popli[1,2&3], and Ramakrishna Kommagani[1,2&3]

[1]Department of Pathology & Immunology, Baylor College of Medicine, Houston, TX 77030, USA, [2]Department Obstetrics and Gynecology, [3]Center for Reproductive Health Sciences

Introduction: Although endometrial cancer is the most common cancer of the female reproductive tract, we have little understanding of what controls endometrial cancer beyond the transcriptional effects of steroid hormones such as estrogen. As a result, we have limited therapeutic options for the ~62,000 women diagnosed with endometrial cancer each year in the United States. Here, to identify new prognostic and therapeutic targets, we focused on a new area for this cancer-alternative mRNA splicing, specifically the role of splicing factor SF3B1.

Method of Study: Using the doxycycline-inducible vector strategy, we stably transfected doxycycline-induced EGFP-tagged SF3B1 shRNA to deplete its levels in AN3CA cells, an endometrial cancer cell line with high endogenous SF3B1 levels. Similarly, RL-95-2 cells with low endogenous SF3B1 levels were transfected with doxycycline-induced EGFP-tagged SF3B1 overexpression vectors. After transduction, both cell lines were subjected to puromycin selection followed by treatment with doxycycline to check the SF3B1 expression status. The overexpressed or depleted SF3B1 levels were first confirmed by Western Blotting. Once established, these stable cells were subjected to a series of cellular assays to identify their tumorigenicity or metastatic potential.

Results: Cellular proliferation assays revealed AN3CA cells with reduced SF3B1 levels had less tumorigenic potential (70% less proliferative) compared to control cells. In contrast, RL95-2 cells with reduced endogenous SF3B1 levels when overexpressed with WT SF3B1 or mutant R957Q vectors became hyper-proliferative and showed a remarkable enhancement in tumorigenic potential (~3-4 fold) compared to control cells. Additionally, wound healing assay analysis revealed AN3CA-SF3B1 shRNA transduced cells had significantly reduced migration potential (~70-80 % less migration) compared to control shRNA transduced cells. While SF3B1 WT or R957Q overexpressed RL95-2 cells were found to show more wound healing ability compared to control cells. In vivo orthotopic models revealed a significant reduction of solid primary tumor with the injection of shSF3B1 stable cells compared to control cells. Further, the control tumors showed a higher expression of Ki67 positive cells compared to shSF3B1 containing tumors.

Conclusion: Our findings suggest SF3B1 play a crucial oncogenic role in driving endometrial tumorigenesis, and these findings may support the development of SF3B1 inhibitors to treat this cancer.

ID# 24

Lethal Neonatal Pulmonary Hypertension in a Patient with Trisomy 21 (T21) and Congenital Portosystemic Shunts

Rachel Guest MD[1], Dilshad Dhaliwal MD[1], Debra Kearney MD[2], Nahir Cortes-Santiago MD, PhD[2], Kalyani Patel MD[2]
[1]Department of Pathology and Immunology; Baylor College of Medicine; [2]Department of Pathology; Texas Children's Hospital

Introduction

Children with Trisomy 21 (T21) have an increased incidence of pulmonary hypertension (PHTN), most often related to intrinsic lung and/or heart disease. Although rare, congenital portosystemic shunts (CPSS) are another cause of PHTN and may be the most common noncardiac vascular anomaly in T21. We report a 2 days old, full-term neonate with T21, CPSS without structural cardiac anomalies.

Case Presentation

The neonate was small for gestational age with oligohydramnios noted at delivery. Fetal growth and amniotic fluid volume were normal by ultrasound at 30 weeks gestational age. He was intubated soon after delivery for severe hypoxic respiratory failure. Dysmorphic features of T21 were noted and chromosomal microarray confirmed the diagnosis. Echocardiography showed patent fetal shunts with right to left shunting, moderately dilated right heart structures, and right to left septal bowing, consistent with suprasystemic PHTN. There was no radiologic evidence of significant lung disease. Persistent respiratory failure with hemodynamic compromise led to death.

Pathology

Postmortem exam confirmed T21 associated dysmorphic features and echocardiographic anatomic findings. Although the lung weight and lung weight:body weight ratio were normal, histologic features suggested pulmonary hypoplasia with variably small lobules and reduced radial alveolar count. In areas, alveolar architecture appeared simplified with double capillary loops, as often seen in T21. No histologic pulmonary vascular hypertensive changes were identified. The liver had gross and histologic features of extrahepatic and intrahepatic CPSS. Portal vein (PV) and central vein branches were dilated with multiple extra and intrahepatic porto-central communications. Multiple shunt channels connected the extrahepatic PV to the inferior vena cava (IVC), with multiple smaller channels connecting the IVC to the hepatic parenchyma and multiple smaller intrahepatic channels connecting the PV to the hepatic veins. The extrahepatic route can be classified as a type 2 (partial) portosystemic diversion while the intrahepatic channels are one of four types of intrahepatic portosystemic shunts that have been described in literature.

Conclusions

Severe PHTN in this neonate, unexplained by the cardiac and pulmonary anatomy, can be attributed to increased right heart and pulmonary blood flow from the CPSS into lungs with a degree of pulmonary hypoplasia. Although CPSS are rare, hepatic/portal vein anatomy should be carefully evaluated in T21 associated PHTN.

ID# 25

Title: The Role of MRI-Guided Biopsy in Breast Cancer Diagnosis and Patient Monitoring – A Single Institutional Analysis

Tania Platero Portillo(1), Hula Taha (1), Meead Swati (1), Sagar Dhamne (1)
Department of Pathology & Immunology, Baylor College of Medicine, Houston, TX

Background:

Magnetic Resonance Imaging (MRI) is a supplementary tool in breast cancer management. It can be used in patients diagnosed with breast cancer for preoperative assessment, surgical planning, contralateral breast screening, staging and monitoring treatment response. However, it has not gained widespread popularity due to its lower specificity, need for additional biopsies, increased time and higher cost. Studies evaluating breast MRI findings, biopsy rates and histopathology in women undergoing MRI after initial diagnosis of breast cancer are lacking. All women with newly diagnosed breast cancer, in-situ or invasive, undergo MRI evaluation at our tertiary-care county hospital. The aim of this study is to determine MRI findings for MRI-guided biopsy, histopathology correlation and the finding's impact on the subsequent surgical management in these women

Design:

We searched our institute's pathology database for patients undergoing MRI-guided biopsy for disease extent evaluation following a new breast carcinoma diagnosis between January 2021 and September 2023. MRI findings, initial biopsy results, MRI-guided biopsy results and clinical management were retrieved from patient charts. The Chi2 test was used for statistical analysis

Results:

This retrospective study included 85 women, 31 (36.4%) <50 years and 54 (63.6%) ≥ 50 years old. On initial biopsy 69 had invasive carcinoma (60 invasive ductal (IDC), 9 invasive lobular (ILC)) and 14 Ductal carcinoma in situ (DCIS). Among those with IDC, 24 (40%) showed mass enhancement (ME), 31 (51.6%) showed non-mass enhancement (NME) and 5 with both. Lesions were ipsilateral in 33, 18 being in the same quadrant. 23 cases had contralateral lesions and 4 were bilateral. Of the 14 women with DCIS, ME was seen in 6 (43%), NME in 6 (43%) and both in 2 (14%). A clinically significant lesion was present in 16 (19%), 14 IDC group (5 IDC, 7 DCIS, 2 atypical ductal hyperplasia), 1 ILC group (1ILC) and 2 DCIS group (2DCIS). Overall, MRI findings resulted in management change in only 1 patient with IDC who had occult contralateral invasive carcinoma resulting in bilateral mastectomy. Finally, patient age was not a significant factor

Conclusion:

Majority of histopathologic findings in patients undergoing MRI-guided biopsy following breast cancer diagnosis are benign. Even when a clinically significant lesion was present, surgical management was altered in only 1 case. Thus MRI, though sensitive, is non-specific even in patients with known breast carcinoma

ID# 26

Clostridium septicum and *C. difficile* Compete for an Intestinal Lipid-rich Environment Lacking in Naturally Evolved Antimicrobial Activity.

Nian Liu[1], Serge Fobofou[1], Nazli Yalcinkaya[1], Sik Yu So[1], Shyam Badu[1], Margaret Conner[2, 3], Qinglong Wu[1], Tor Savidge[1]

[1]Department of Pathology & Immunology, Baylor College of Medicine, Houston, Texas, USA
[2]Department of Molecular Virology and Microbiology, [3]Department of Education, Innovation and Technology, Baylor College of Medicine, Houston, Texas, USA

Clostridium septicum is a gram-positive, toxin-producing bacterium known to cause gas gangrene. Infection is thought to involve hematogenous dissemination from the intestine, although colonization rates in humans remain poorly understood. To investigate susceptibility risks linked to *C. septicum* colonization, we conducted an extensive metagenomic survey of over 35,000 healthy and patient fecal specimens and observed that *C. septicum* in adults was exceptionally rare. However, intriguingly, this organism was commonly detected in infants. Furthermore, in-depth metagenomic characterization of the infant gut microbiome revealed a shared community representation between *C. septicum* and *C. difficile* colonization. Notably, the absence of shared taxa in this context conferred protection in experimental models of *C. difficile* infection. To substantiate the existence of a competitive gut niche shared by these diverse pathogens, we established an oral model of *C. septicum* infection. We demonstrated that asymptomatic carriage of *C. difficile* completely abrogated clinical disease caused by toxigenic *C. septicum*. Employing an integrated multi-omics approach, we identified a specialized intestinal niche, enriched in ceramides, sphingolipids, and sterols, that is commonly inhabited by these pathogens. Particularly, ceramides represent a key intermediate in sphingolipid biosynthesis known to facilitate host-pathogen interactions. Through comprehensive metagenomic comparisons and bioactivity-guided analysis of key microbiota taxa associated with pathogen decolonization, we successfully identified and elucidated the structure of hadromycin, a novel ether-class of sphingolipid possessing broad antimicrobial activity against *C. septicum* and *C. difficile*. Thus, sphingolipids have evidently evolved in the natural design of clostridial pathogen evasion during human development.

Acknowledgements: Gut Check Foundation, P01-AI152999, U01-AI24290

ID# 27

Eppin and Closely Related WAP Four-disulfide Core Genes _Wfdc6a, Wfdc8, and Wfdc6b_ Impact Sperm Differentiation and Male Fertility in Mice.

Katarzyna Kent[1,2,3], Kaori Nozawa[1,2], Rachel M. Parkes[1,2], Laura Dean[1,2], Mei Leng[4], Antrix Jain[4], Anna Malovannaya[4,5], Martin M. Matzuk[1,2,3], Thomas X. Garcia[1,2,6,*]

[1]Center for Drug Discovery, Baylor College of Medicine;
[2]Department of Pathology & Immunology, Baylor College of Medicine;
[3]Department of Molecular & Human Genetics, Baylor College of Medicine;
[4]Mass Spectrometry Proteomics Core, Baylor College of Medicine;
[5]Verna and Marrs McLean Department of Biochemistry and Molecular Biology, Baylor College of Medicine;
[6]Scott Department of Urology, Baylor College of Medicine.

Despite 96 million years of evolution separating humans and rodents, eleven closely-related reproductive tract-specific genes in humans—*SPINT3*, *WFDC6*, *EPPIN*, *WFDC8*, *WFDC9*, *WFDC10A*, *WFDC11*, *WFDC10B*, *WFDC13*, *SPINT4*, and *WFDC3*—and the thirteen reproductive tract-specific orthologous genes in mice, form highly conserved gene clusters indicative of conserved, combined critical functions in the male reproductive tract. However, despite advancements towards a non-hormonal male contraceptive targeting EPPIN, none of the closely related genes within the WFDC locus have been functionally explored through genetically manipulated mouse models. In this study, we sought to clarify the involvement of the entire locus of reproductive tract specific WFDC genes in male fertility. To avoid potential gene redundancy effects in single gene knockouts (KOs), we generated mice lacking a combined total of thirteen (*S13/W3*), ten (*S13/W13*), five (*W16/W13*), or four (*W6a/W6b*) genes within the conserved gene cluster using CRISPR/Cas9-electroporation of zygotes (CRISPR-EZ) gene editing technology. Reproductive phenotype analysis of resulting KO and WT littermates revealed that *W16/W13* KO males were infertile due to reduced sperm motility and increased sperm death, while *S13/W3*, *S13/W13*, and *W6a/W6b* KO males displayed severe infertility characterized by decreased testes size with reduced epithelial thickness and absence of mature sperm (azoospermia) due to defects in spermatid development. Specifically, *W6a/W6b* KO mice

–continued on page 43

– *continued from page 42*

lacking protease inhibitors encoded by *Wfdc6a, Eppin, Wfdc8, and Wfdc6b* exhibited impaired spermatid differentiation from round to elongated spermatids. To identify direct targets affected by the absence of the WFDC protease inhibitors, rather than generating a proteomic signature primarily influenced by the absence of elongated spermatids, we conducted a proteome profiling analysis of whole testes at the early postnatal age of 28 days when elongated spermatids are just initiating their development in mouse testes. Our analysis revealed altered expression of various proteins in KO testes including upregulation of serine/threonine proteases, and cell cycle, apoptosis, and meiosis regulator proteins, such as CCDC42, STRA8, ZFY1 and ZFY2, indicating a compensatory response to increased protease activity in the testes. Downregulated proteins included structural and epigenetic regulatory proteins and protease inhibitors, likely resulting from excessive protease activity in *W6a/W6b* KO mice, leading to abnormal processing or degradation of key proteins required for spermatid development such as TSSK3, SRM, SPATS1, and SPATA proteins. Our studies, the first to explore an entire WFDC locus of closely related genes, not only clarified the functional requirement of WFDC locus genes in male fertility but also shed light on the involvement of EPPIN and its closely related WFDC proteins as key protease inhibitors regulating various proteolytic processes essential for the normal progression of spermatogenesis, particularly affecting the transition from round to elongated spermatids essential for sperm development. These findings have implications for improving clinical diagnoses of male infertility and development of novel contraceptive strategies. This study has been supported by the National Institutes of Health (NIH) trainee award T32GM139534 and the A.I. & Manet Schepps Discovery Foundation fellowship (to K.K.); and NIH awards R01HD106056 and R01HD095341 and the Male Contraceptive Initiative David Sokal Innovation award 2021-302 (to T.X.G.).

ID# 28

Hi-C Metagenomic Characterization of the Host-Antimicrobial Resistome in *Clostridioides difficile* Infection.

Henok A. Tegegne[1], Ben Auch[2], Shyam Badu[1], Prapaporn Boonma[1], James Dunn[1], Kevin Garey[3], Samuel Shelbourne[4], Cesar Arias[5], Todd Treagen[6], Blake Hanson[7], Ivan Liachko[2], Tor C. Savidge[1]

[1]Department of Pathology & Immunology, Baylor College of Medicine; [2]Phase Genomics; [3]Department of Pharmacy Practice and Translational Research, University of Houston; [4]Department of Infectious Diseases, Infection Control, and Employee Health, MD Anderson Cancer Center; [5]Department of Internal Medicine, Division of Infectious Diseases, Houston Methodists; [6]Department of Computer Science, Rice University; [7]Department of Epidemiology, Human Genetics & Environmental Sciences, UTHealth

Corresponding author: Henok Ayalew Tegegne, Department of Pathology & Immunology, Baylor College of Medicine. E-mail: henok.tegegne@bcm.edu

Objective: This study employed Hi-C metagenomics to investigate clinically significant features in *Clostridioides difficile* infection (CDI) and corresponding antimicrobial resistance (AMR) profiles. Our primary goal was to characterize the genetic composition of gut microbiome communities, with specific attention paid to identifying mobile genetic elements (MGEs) and their associated AMR genes, utilizing the Hi-C metagenomic approach.

Methods: Fecal specimens from 10 pediatric subjects, including 5 CDI cases with prior antibiotic treatment and 5 healthy age-matched controls, underwent comprehensive analysis using the ProxiMeta™ Platform. In addition to ProxiMeta, widely used metagenome assembled genome (MAG) tools such as bin3c, MetaBAT2 and MetaPhlan4 were employed for comparative analysis. Marker gene detection involved BLAST searches, followed by network analyses utilizing Hi-C connectivity graphs. The identification of AMR genes and plasmids was conducted using AMRFinder Plus and BLAST against the RefSeq plasmid database. Our integrated approach linked plasmid, AMR, and virus contigs to genome clusters, while taxonomic summaries provided insights into host microbiome interactions.

Results: ProxiMeta2 successfully recovered a total of 304 complete MAGs (>95% completeness; <10% contamination). Taxonomic profiling revealed discernible shifts in the gut community structure of CDI samples, characterized by a reduction in *Lachnospiraceae* and *Ruminococcaceae*, and the prevalence of *Enterococcaceae*. AMR analysis identified up to 132 resistance genes per sample, with CDI samples exhibiting higher abundance, highlighting the pivotal role of plasmids in the dissemination of AMR. Host taxa predominantly linked with AMR genes included *Clostridiales* and *Bacteroidales*. Distinctive profiles in a CDI sample (bf12_860557) also indicated potential adaptation to environmental pressures, showcasing the versatility of AMR genes. Moreover, our study identified a significant connection between *Enterobacteriales* and resistance genes against heavy metals and disinfectants, as well as unveiling pathogenicity loci in *C. difficile* and virulence factors in *S. aureus*.

Conclusion: Hi-C metagenomics is emerging as a transformative new tool to define the specific role of select gut taxa in maintaining and propagating a diverse AMR landscape. Further, our studies highlight the significant role of *Enterobacteriales*-derived plasmids in transferring resistance genes in response to environmental selective pressures.

Acknowledgements: Funded by the National Institute of Allergy and Infectious Diseases (NIAID), T32 AI141349

ID# 29

Transfusion Thresholds in Pediatric Critical Care: A Retrospective Database Review

Sulakshana Ranjan, M.D.[1] and Thomas Chong, M.D.[2] [1,2]Department of Pathology & Immunology; Baylor College of Medicine, Clinical Informatics Division

Introduction:

Mounting evidence supports lower hemoglobin thresholds in blood transfusions. This retrospective study at Texas Children's Hospital investigates transfusion strategies in stable, critically ill children using our hospital's electronic health record (EHR) databases, namely, Wellsky's Transfusion and Epic's Clarity databases. Based on findings from Lacroix *et al.*'s trial, we hypothesize that a hemoglobin threshold of 7 g/dL can decrease transfusion requirements without increasing adverse outcomes.

Methods:

Conducting a retrospective review from December 2010 to October 2023, we utilize Clarity and Wellsky databases. The study includes male and female in-patients aged ≥ 29 days receiving blood at a hemoglobin threshold of 7 g/dL (restrictive) or 9.5 g/dL (liberal) in the Pediatric Intensive Care Unit. The threshold at which transfusion took place was inferred by retrospectively looking at the hemoglobin result just prior to initiation of transfusion. Clinical data from Epic Clarity includes diagnoses, laboratory data, and mortality, while blood product transfusion information is extracted from the Wellsky Transfusion database. Calculations include 30-day mortality rates, Kaplan–Meier curves, and determining the Pediatric Multiple Organ Dysfunction Score (P-MODS).

Results:

Preliminary results reveal a higher mortality rate in the liberal transfusion group, indicating potential adverse outcomes. Comprehensive analysis involves calculating 30-day mortality rates, plotting Kaplan–Meier curves, and determining the 95% confidence interval for absolute risk reduction. Differences in the average Pediatric Multiple Organ Dysfunction Score (P-MODS) are assessed, highlighting potential implications for patient outcomes.

Conclusions:

The study suggests that a hemoglobin threshold of 7 g/dL may be associated with decreased mortality and improved outcomes compared to a 9.5 g/dL threshold in stable, critically ill children. These findings align with the hypothesis and Lacroix *et al.*'s trial. While not a replacement for randomized controlled trials, retrospective database reviews offer an opportunity to generate evidence that complements and strengthens our understanding of clinical practices and outcomes, particularly in situations where conducting prospective trials may be challenging or impractical.The study underscores the importance of reevaluating transfusion strategies, especially in vulnerable populations, and emphasizes the significance of real-world data in optimizing pediatric transfusion practices.

ID# 31

A System for Controlling Mammalian Gene Expression via the Modulation of Poly-A Signal Cleavage at 5'UTR

Jocelyn D-Y. Jea, Liming Luo, Yan Wang, Pei-Wen Chao, Laising Yen

Department of Pathology & Immunology, Department of Molecular and Cellular Biology, Dan L. Duncan Cancer Center, Baylor College of Medicine

The ability to control gene expression in mammalian cells is crucial for safe and efficacious therapies, and for elucidating gene functions. Current gene regulation systems for mammalian cells either elicit harmful immune responses or lack the regulatory efficiency. As a result, none has been approved by the FDA for clinical use.

Here, we describe the 'pA regulator', an RNA-based switch that controls mammalian gene expression through poly-A signal (PAS) cleavage at 5' UTR. First, a synthetic PAS is introduced into the 5'UTR of the target gene to generate efficient cleavage and subsequent degradation of the mRNA, resulting in the loss of gene expression. Second, specific ligand binding to the aptamer, an RNA 'sensor' sequence surrounding PAS, inhibits the cleavage, thereby preserving the intact mRNA and inducing gene expression. To achieve exceptional control, the cleavage of PAS is modulated by a 'dual-mechanism': (1) drug binding that directly inhibits the PAS cleavage and (2) drug-induced alternative splicing that removes the PAS, both activated by drug administration to cells.

This RNA-based system circumvents the immune responses that plague other systems, and achieves up to 900-fold induction with an EC_{50} of 0.5 µg/ml Tetracycline, which is well within the FDA-approved dose range. The pA regulator effectively controls eGFP transgene in stable cell lines, luciferase transgene in live mice by AAV-mediated gene transfer, and the endogenous *CD133* gene in human genome, in a dose-dependent and reversible manner with long-term stability.

Gene regulation in clinical settings requires demanding features of non-immunogenicity, high dynamic ranges, low leakage expression, and low ligand concentrations for induction. The pA regulator fulfills such needs and achieves an unprecedented regulation by using an FDA-approved drug within the clinically safe dose range. As such, we envision that the pA regulator could have wide-ranging applications both in biological studies and clinical settings.

ID# 33

Integrated Characterization of Soft Tissue and CNS CIC-Rearranged Sarcomas Reveals Shared Epigenetic Signatures Across Fusion Types and Anatomic Locations

J Van Arnam; F Lin, W Parsons, A Major, M Shafiekhani, H Voicu, M Hicks, K Patel, D Lopez-Terrada, K Fisher; C Mohila, M Blessing, A Roy

Texas Children's Hospital, Baylor College of Medicine Department of Pathology and Immunology, Houston TX USA

CIC-rearranged sarcoma is a high-grade undifferentiated sarcoma defined by *CIC* fusions with *DUX4* or less common non-*DUX4* partners. While the majority arise in soft tissue (ST), primary *CIC*-rearranged sarcomas are also reported in the central nervous system (CNS). While known to share histopathologic, genetic, and clinical features, it remains unclear if *CIC*-rearranged sarcomas from diverse locations and varied fusion partners are epigenetically related. We sought to characterize a set of *CIC*-rearranged sarcomas in an integrated fashion by examination of their histologic, immunophenotypic, and molecular findings including methylation profiling classification.

Texas Children's Hospital (TCH) pathology archival search identified *CIC*-rearranged sarcomas as detected by TCH Solid Tumor next-generation sequencing panel. Whole transcriptome sequencing (RNA-seq) of previously uncharacterized undifferentiated sarcomas or DNA methylation profiling identified additional cases. RNA-seq libraries were sequenced (2×100-bp reads) and analyzed by ensemble fusion callers. Tumor DNA methylation profiling was conducted with Infinium MethylationEPIC arrays (Illumina) and analyzed with the DKFZ neuropathology classifier version 12.5. Histomorphology and available immunostains were reviewed, blinded to the *CIC* mutation.

We identified 25 cases from 13 patients (8 male, 5 female). Eleven presented with a ST primary, and 2 as CNS tumors. Of these, 19 cases from 12 patients ages 5-17 were available for review. Of the 11 ST cases, 10 had *CIC::DUX4* fusions and one had a *CIC::FOXO4* fusion. The 2 CNS cases harbored one each of *CIC::NUTM1* and *CIC::LEUTX* fusion. Two histomorphologic patterns predominated: a densely cellular "Ewing-like" pattern with scant stroma and primarily round to ovoid cells with high N:C ratio, and another with myxoid stroma where tumor cells demonstrate eccentrically located nuclei with eosinophilic cytoplasm. One case, a left frontal lobe primary with *CIC::LEUTX* fusion, showed sheets of ganglion-like cells. When performed, at least partial CD99 staining was observed, sometimes dot-like; two cases from different patients were WT1-negative. Methylation profiling performed on 7 cases (5 soft tissue, 2 CNS) showed all cases with different *CIC* fusions to co-cluster as *CIC*-rearranged sarcomas.

Despite varied locations, morphologic and immunophenotypic features and fusion partners, methylation profiling demonstrates clustering of both ST and CNS CIC-fused sarcomas. Given CIC's role as a transcriptional repressor, profound changes induced by its alteration may overwhelm prior methylation states present in the original cell of origin. These results further reinforce the need for molecular classification of Ewing-like neoplasms for final diagnosis in all body sites.

– *continued on page 48*

– *continued from page 47*

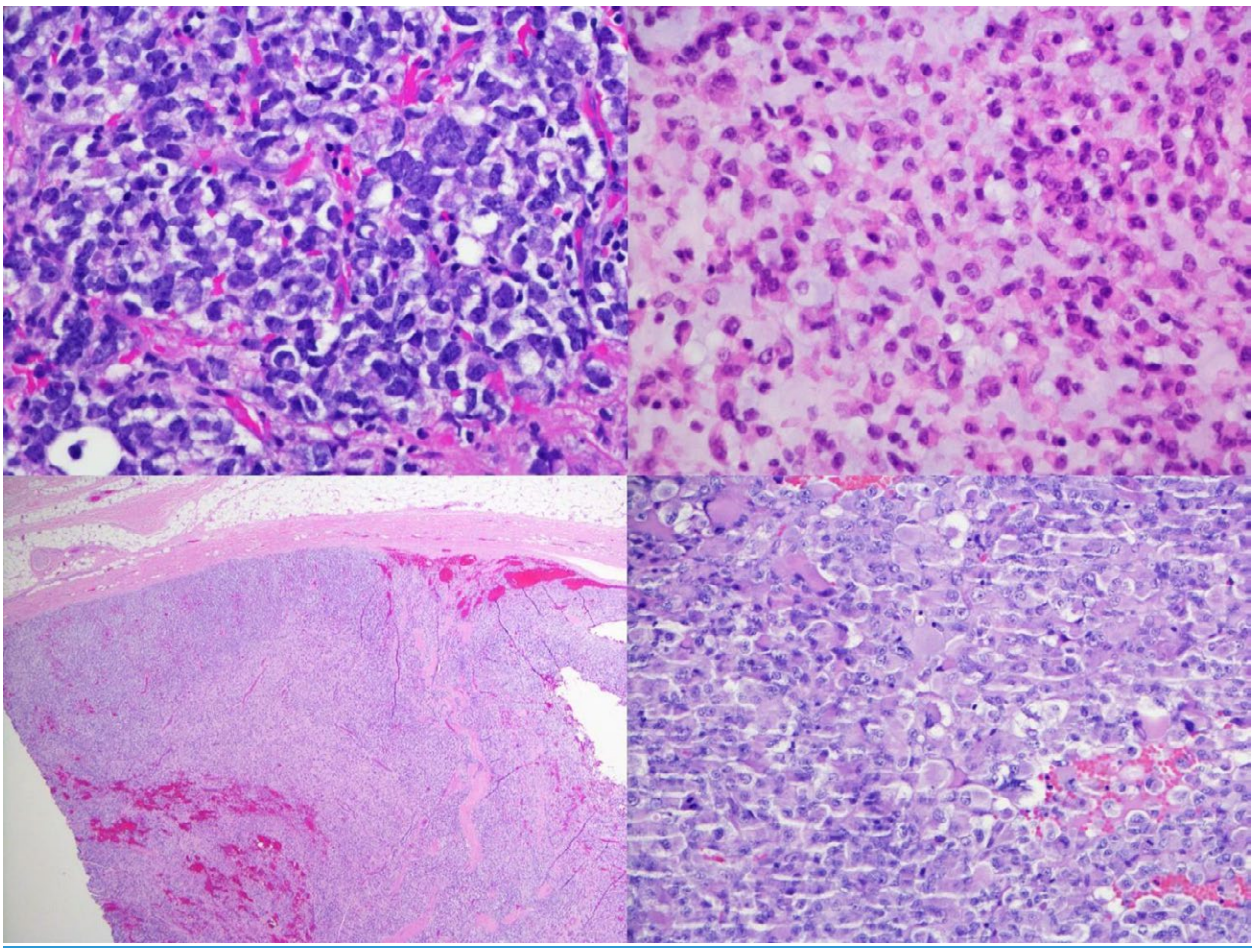

ID# 34

Dendritic cell-intrinsic AIMp1 regulates type 1 immune polarization through p38 MAPK and AP-1 signaling

Keenan Ernste[1,2], Dan Liang[1,2], Briana Burns[1,2], Sharon Amanya[1,2], Giselle De La Torre Pinedo[1,2], Jonathan Vasquez-Perez[1,2], Damilola Oyewole-Said[1,2], Nalini Bisht[1,2], Vanaja Konduri[1,3], William K. Decker[1,3,4]

[1]Department of Pathology and Immunology; [2]Graduate School of Biomedical Sciences; [3]Dan L. Duncan Comprehensive Cancer Center; [4]Center for Cell and Gene Therapy (CAGT), Houston, TX 77030, USA

Introduction

Dendritic cells (DCs) are responsible for initiating adaptive immunity by interpreting environmental signals and tailoring the downstream immune responses to combat pathogens most effectively in a process known as adaptive immune polarization. The precise molecular mechanisms regulating DC-mediated immune polarization are incompletely understood and defining them is critical for understanding how DCs contribute to disease resolution. This is especially true in cancers, which actively antagonize DC-mediated immune activation and polarization. Recent studies suggest that the cytokine AIMp1 is critical for promoting type 1 immune polarization and is associated with favorable long-term outcomes in diverse cancers. Work from our group suggests DC-intrinsic AIMp1 drives complete DC polarization to promote cellular immunity, thereby optimally activating T helper type 1 cell responses and efficient immune responses in models of melanoma and influenza infection. Building on that work, we investigated DC signaling pathways that may be regulated by AIMp1.

Methods

To broadly investigate differences in protein expression and phosphorylation events in major cell signaling pathways, reverse phase protein array (RPPA) analysis was performed using AIMp1 knockout (AIMp1 KO) and wild-type (AIMp1 WT) mouse bone marrow-derived dendritic cells (BMDCs) stimulated with LPS. Western blotting and pharmacological inhibition of protein signaling intermediates to validate specific protein signaling pathways dysregulated in AIMp1 KO cells.

Results

Findings revealed that DCs lacking AIMp1 exhibit impaired p38 MAPK signaling, failing to adequately upregulate phospho-p38 MAPK in response to stimulation. This impairment was specifically observed at the level of p38 MAPK itself, since the loss of AIMp1 did not affect phosphorylation of the kinase upstream of p38 MAPK, MKK3/6, but did affect the p38 MAPK target protein MAPKAPK2. As expected based on these results, we also observed significant dysregulation of the AP-1 transcription factor subunits c-Fos and c-Jun in AIMp1 KO cells. Furthermore, pharmacological inhibition of one of the major p38 MAPK phosphatases, PP2A, rescued the phosphorylation of p38 MAPK in AIMp1 KO cells along with their ability to stimulate T cell IFNγ production to a similar level as that observed in AIMp1 WT cells. Finally, AIMp1 KO cells also had dysregulated expression of two of the major PP2A inhibitors, ANP32A and SET.

Conclusions

Our results revealed that AIMp1 plays a significant role in promoting efficient p38 MAPK phosphorylation and signaling in mouse BMDCs, which may in turn be an important precursor step to proper dimerization and transcriptional regulation of AP-1 transcription factors following stimulation. Furthermore, PP2A was identified as a putative phosphatase responsible for lower p38 MAPK phosphorylation in AIMp1 KO BMDCs. Although the direct protein-protein interactions through which AIMp1 exerts its effects on PP2A and p38 MAPK signaling are still unknown, previous studies have identified that AIMp1 may directly interact with ANP32A and SET, the two major nonredundant negative regulators of PP2A, which is supported by our results showing that both ANP32A and SET are dysregulated in AIMp1 KO DCs. Altogether, this work underscores the importance of AIMp1 in immune polarization and offers potential molecular targets for modulating DC function in disease.

ID# 35

EBV-Positive Inflammatory Pseudotumor Follicular Dendritic Cell Sarcoma: Rare Atypical Presentation in the Spleen

Nicole Y. Wang[1], Fouad El-Dana MD[2], Ya Xu, MD, PhD[2], Natalia Golardi, MD[2]

Departments of [1]Medical Scientist Training Program (MSTP) and [2]Pathology & Immunology, Baylor College of Medicine, Houston, TX.

EBV-positive inflammatory follicular dendritic cell (FDC) sarcoma is a rare indolent malignant neoplasm involving liver and spleen with occasional involvement of colon, pancreas and mesentery. The etiology is strongly associated with EBV. Clinical presentation is non-specific including anemia, hypoalbuminemia, hypergammaglobulinemia and peripheral eosinophilia. Here we present a case of splenic EBV+ inflammatory FDC sarcoma with atypical features.

The patient is a 26-year-old male, who presented with back pain, anemia and hypergammaglobulinemia, and was discovered to have an incidental 11.5 cm splenic mass on MRI. The patient underwent splenectomy. Grossly, the spleen was markedly enlarged measuring 19 cm with well-demarcated large 11 cm mass with cystic spaces and areas of necrosis. Microscopically, the lesion was comprised of polymorphous lymphoplasmacytic infiltrate with scattered multinucleated giant cells and ovoid stromal cells with patchy coagulative necrosis and without mitosis. No fascicles/clusters of spindle cells were seen, which was unusual/atypical for this entity.
By immunohistochemistry, multinucleated and ovoid stromal cells were strongly positive for EBER in situ hybridization (ISH) positive for smooth muscle actin (SMA), very rare cells positive for follicular dendritic cell markers (CD21, CD23), and negative for ALK-1, B- and T-cell markers. Plasma cells were polytypic by Kappa and Lambda ISH. The background small lymphocytes were B- and T-cells with predominance of $CD4^+$ T-cells. Final diagnosis of EBV-positive inflammatory FDC sarcoma was rendered.

Given its nonspecific clinical presentation and imaging characteristics, absence of significant spindle cell component in fascicular pattern that usually comprises a significant part in this entity, made diagnosis especially challenging.

ID# 37

Pitfall of Positive DDIT3 Fluorescent in Situ Hybridization in Spindle cell/pleomorphic Lipoma: A Case Series

Dorsay Sadeghian MD[1], Peyman Dinarvand MD[1]

1 Department of Pathology, Baylor College of Medicine, Houston, Texas

Introduction:

Spindle cell/pleomorphic lipoma is a benign tumor, primarily affects middle aged men. This lesion is characterized by a variable number of mature adipocytes, intermixed with bland looking spindle cells. Stromal myxoid changes and occasional atypical lipoblast-like cells may be observed. The presence of these histo-morphological features may resemble differential diagnosis such as myxoid liposarcoma which is a malignant tumor with significant risk of recurrence and metastasis. This resemblance may lead to ordering tests to detect a gene fusion involving DNA Damage Inducible Transcript 3 (DDIT3), which is a sensitive and specific marker for myxoid liposarcoma.

Case Presentation:

We discuss two cases with nasal masses who were taught to be myxoid liposarcoma (given the histo-morphological overlaps) under microscope, and therefore DDIT3 Fluorescent in Situ Hybridization (FISH) were ordered. The percentage of cells with an abnormality exceeds the normal cutoff (marginally exceeded) in both cases in DDIT3 FISH and both cases were taught to be myxoid liposarcoma on initial evaluation.

Pathology:

Given the unusual location for myxoid liposarcoma, further evaluation by Next Generation Sequencing (NGS) for sarcomas was performed, which revealed no gene fusion for DDIT3. These results followed by immunohistochemical staining for CD34 and Retinoblastoma Protein 1 (RB1), which exhibited strong and diffuse CD34 staining and loss of nuclear RB1 in the tumor spindle cells, proved the diagnosis as spindle cell/pleomorphic lipoma.

Conclusion:

This case series reports, for the first time, that spindle cell/pleomorphic lipoma can have DDIT3 rearrangement on FISH studies and that can be a pitfall if further studies are not performed.

ID# 39

Liver Arteritis: An Uncommon Etiology of Ischemic Cholangiopathy With Primary Sclerosing Cholangitis-like Histologic Features

Dorsay Sadeghian MD [1] , Sadhna Dhingra MD [2] , Saira Khaderi MD, MPH [3] , Shilpa Jain MD [1]

1. **Department of Pathology, Baylor College of Medicine, Houston, Texas**
2. **Department of pathology Houston Methodist, Houston, Texas**
3. **Department of Medicine, Baylor College of Medicine, Houston, Texas**

Ischemic cholangiopathy is a condition characterized by focal or diffuse damage to bile duct, resulting from impaired blood supply, which may exhibit variable histologic features. While this concept is well described in post-liver transplant patients, other causes of small hepatic artery injury may lead to ischemia and bile duct damage. Although it is extremely uncommon, involvement of liver as part of systemic or isolated vasculitis can lead to microvasculature damage.

We are describing a case of ischemic cholangiopathy attributed to isolated liver arteritis, in a 49 y/o lady presented with increase in alkaline phosphatase (1237 U/L) and gamma-glutamyl transferase (700 U/L), along with elevated erythrocyte sedimentation rate and C-reactive protein. Microscopic examination of liver biopsy revealed portal tracts with edema, mild lymphocytic infiltration, and peri-ductal fibrosis, mimicking sclerosing cholangitis. There was no interface hepatitis, ductular reaction or ductopenia (Figure A-C). Focus of necrotizing granulomatous arteritis, zone 3 sinusoidal dilatation and hepatocyte atrophy were seen.

Further evaluation of the patient revealed no positive serologic markers. Magnetic resonance cholangiopancreatography showed unremarkable intra- and extrahepatic bile ducts. Immunosuppressive treatment resulted in significant alkaline phosphatase decrease, and partial resolution of histologic features upon follow-up biopsy (Figure D)

In conditions with chronic blood supply disruption such as arteritis, histologic features may resemble pathologies with permanent bile duct damage. In reversible scenarios like arteritis, a precise diagnosis and intervention can potentially avert enduring complications such as ductopenia and fibrosis. This case report sets the groundwork for further research on the link between vasculitis and liver injury.

ID# 40

TPM3-NTRK1 Fusion Uterine Cervical Sarcoma: A Case Report of a Rare Entity

Isha Khanduri MD[1], Dorsay Sadeghian MD[1], Ramya P. Masand MD[1]

[1]Department of Pathology, Baylor College of Medicine, Houston

Introduction: Sarcomas of the cervix constitute less than 1% of all cervical malignancies, with rhabdomyosarcomas being the most reported sarcomas. Most patients present with vaginal bleeding and a bulky cervical mass at diagnosis. Due to their diverse and overlapping histology, ancillary techniques are necessary for definitive diagnosis. We report a case of TPM3-Neurotrophic tyrosine kinase 1 (NTRK) fusion cervical sarcoma in a postmenopausal woman.

Case Presentation: A 50-year-old woman presented with postmenopausal bleeding. Ultrasonography revealed leiomyomatous uterus. The patient underwent hysterectomy with bilateral salpingo-oophorectomy.

Pathology: On microscopy, an incidental tumor circumferentially replacing cervical stroma with pushing and focally infiltrative borders with entrapped endocervical glands was identified (Figures 1A, 1B and 1C). The tumor was composed of haphazardly arranged uniform spindle cells in vague myxoid background with low mitotic index and brisk lymphocytic infiltrate (Figure 1D). Differential diagnosis of adenosarcoma and inflammatory myofibroblastic tumor was considered. The tumor cells were negative for smooth and skeletal muscle markers, and ALK1, with patchy positivity for CD10 and Cyclin D1. Given the non-specific low grade morphology, next-generation sequencing was performed and revealed a TPM3-NTRK1 fusion.

Conclusions: NTRK rearranged uterine sarcomas are recently described with activating mutations of NTRK, TPM3:NTRK1 being the most common fusion. Unusual adenosarcoma-like/fibrosarcoma-like spindle cell neoplasms of the cervix may represent NTRK fusion sarcoma, which can be detected by S100 and pan-Trk staining and confirmed by NTRK molecular testing. This entity must be differentiated from malignant peripheral nerve sheath tumors, inflammatory myofibroblastic tumor with ETV6-NTRK3 fusion and COL1A1-PDGFB fusion sarcomas due to availability of targeted therapy.

ID# 41

STK11 Mutated Adnexal Tumor: An Emerging Entity

Isha Khanduri MD[1], Dorsay Sadeghian MD[1], Ramya P. Masand MD[1]

[1]Department of Pathology, Baylor College of Medicine, Houston

Introduction: STK11-mutated adnexal tumors represent a recently described, distinct category of locally infiltrative neoplasms, predominantly in the para-tubal region with an aggressive clinical course. They manifest diverse morphological patterns and harbor characteristic STK11 gene mutations, loss of heterozygosity being the most common. Considering overlapping histologic features with sex-cord stromal tumors and tumors of wolffian origin, morphologic categorization of these tumors poses significant diagnostic challenges.

Case Presentation: We describe a case of a 45-year-old woman with acute lower abdominal pain with the clinical suspicion of ovarian torsion. The patent underwent right salpingo-oophorectomy showing a 14 cm hemorrhagic para-tubal cystic mass.

Pathology: On microscopy, epithelioid neoplastic cells were arranged in diverse architectural patterns including glandular and tubular structures along with anastomosing corded, reticular and solid patterns (Figures A-D). Moderate mitotic activity was noted with proliferation index of 20%. Immunohistochemical staining exhibited patchy positivity for sex cord markers calretinin, CD56, as well as ER, PR and CD117. Inhibin, cytokeratin, PAX8, EMA, WT-1, synaptophysin, chromogranin, GATA-3, SALL4, SF-1 and PAX2 were negative. Differential diagnosis of female adnexal tumor of wolffian origin and sex-cord stromal tumors were considered. Subsequent evaluation by next generation sequencing identified a possible germline STK11 mutation.

Conclusions: This case highlights the significance of adopting a comprehensive approach, including integration of genomic analysis, to reveal the presence of STK11 gene alterations, in unclassified adnexal tumors demonstrating heterogeneous histologic patterns. Identification of STK11 mutation, despite overlapping immunohistochemical profiles with other tumors aids in accurate classification and patient management, given the aggressive behavior of these tumors.

ID# 43

Title: The Importance of Comprehensive Evaluation of Thyroid Lesions Including Low-Risk Thyroid Neoplasms in Identifying *PTEN*-Related Clinical Syndromes

Angelina S. Bortoletto PhD[1], Donghwa Baek MD[2], Pisey R. Talbott MD[3], Bettye Cox MD[3], Ya Xu MD, PhD[3]

Departments of [1]Medical Scientist Training Program (MSTP) and [3]Pathology & Immunology, Baylor College of Medicine; [2]Department of Pathology & Genomic Medicine, Houston Methodist Hospital

Introduction: Follicular tumors of uncertain malignant potential (FT-UMP) and non-invasive follicular thyroid neoplasms with papillary-like nuclear features (NIFTP) are considered low-risk thyroid neoplasms. NIFTP, but not FT-UMP, in the context of *PTEN*-related clinical syndromes, has been reported in very few studies. *PTEN*-related clinical syndromes predispose individuals to multiple neoplasms and require lifelong cancer screening. Here we report two cases of thyroid neoplasms with loss of PTEN expression.

Case Presentation: The first patient was a 45-year-old female with a family history of thyroid neoplasms, presenting with symptomatic multinodular goiter. She underwent a total thyroidectomy. The second patient was a 36-year-old female referred for genetic testing after her autistic daughter was confirmed to have a germline mutation in *PTEN*. Genetic testing of the patient also revealed a heterozygous pathogenic germline mutation in *PTEN (*c.263_264delAT, p.Y88Sfs*3). Upon screening, she was found to have a subcentimeter breast mass, a 1.5 cm parotid mass, and multiple thyroid nodules by imaging. Identification of these masses in the setting of the *PTEN* mutation led to a diagnosis of Cowden syndrome (CS), which is one of the *PTEN*-related clinical syndromes. A breast biopsy, superficial parotidectomy, and total thyroidectomy were performed.

Pathologic Findings: Histologic examination of the first patient's thyroid specimen showed multiple follicular adenomas and a FT-UMP in a background of thyroid follicular nodular disease. Immunohistochemistry illustrated a follicular adenoma with loss of PTEN expression, and genetic testing for *PTEN* mutation was suggested (patient lost to follow-up). The FT-UMP demonstrated *EIF1AX* mutation (p.G9D, c.26G>A) by molecular testing. For the second patient, an invasive ductal carcinoma was identified by breast biopsy and an oncocytoma was present in the parotidectomy specimen. The total thyroidectomy specimen displayed multiple follicular adenomas, a papillary thyroid carcinoma, and a NIFTP, with loss of PTEN expression by immunohistochemistry.

Conclusion: This study emphasizes the need for a comprehensive evaluation of all thyroid lesions/nodules and testing for PTEN expression to identify *PTEN*-related clinical syndromes. Furthermore, this study supports the inclusion of low-grade thyroid nodules as manifestations in the broad spectrum of neoplasms associated with *PTEN*-related clinical syndromes. This report also demonstrates that NIFTP, but not FT-UMP, is associated with *PTEN* mutations. Finally, to the best of our knowledge, parotid oncocytomas, which are uncommon and benign salivary gland neoplasms, have not been previously reported in Cowden syndrome. In summary, the findings we reported here should encourage clinicians to consider CS and other PTEN-related clinical syndromes in the differential diagnoses.

ID# 44

Dedifferentiated Liposarcoma (28 cm) with Extensive Rhabdoblastic Differentiation – A Challenging Case Disguised Twice on Biopsies

William YY. Wu[1], Amber V. Carrillo MD[2], Chris Finch MD[2,3], Neda Zarrin-Khameh MD[2,3], Ya Xu MD, PhD[2,3]

[1]Medical Scientist Training Program (MSTP) and [2]Department of Pathology & Immunology, Baylor College of Medicine, Houston, Texas

[3]Department of Pathology & Laboratory Medicine, Ben Taub Hospital, Harris Health System, Houston, Texas

Introduction: Dedifferentiated liposarcoma (DDLPS) can be challenging to diagnose histologically, and may heterologously differentiate into various sarcomas, as this study illustrates.

Case Presentation: A 44-year-old man presented with abdominal distension over one month, and was found to have a large retroperitoneal mass by imaging. Rhabdomyosarcoma was reported on an initial biopsy. The tumor progressed despite neoadjuvant chemotherapy. Repeat biopsy showed high-grade sarcoma. Subsequent radical resection with left nephrectomy and left colectomy was performed.

Pathology: The initial biopsy showed a mitotically active spindle cell tumor, with an immunostaining pattern (Desmin +, Myogenin +, MyoD1 +) of rhabdomyosarcoma. Repeat biopsy demonstrated predominantly pleomorphic tumor cells, exhibiting a different immunostaining pattern (Desmin +, Myogenin -, MyoD1 -). The resection specimen grossly showed multiple large masses (28 to 50 cm) focally wrapping the left kidney, and numerous smaller masses in the left colon mesentery. Microscopically, the tumor contained heterogeneous architecture including spindle cells in fascicles admixed with rhabdoblasts, and features of well-differentiated liposarcoma (WDLPS), with rare lipoblasts. The tumor involved the superficial renal parenchyma, mesentery, and colonic serosa. The pleomorphic cells among adipocytes displayed Desmin positivity. *MDM2* amplification was detected in the tumor by fluorescence in situ hybridization. Final diagnosis of DDLPS with extensive rhabdoblastic differentiation arising from WDLPS was rendered.

Conclusions: This report highlights the importance of ruling in/out DDLPS when evaluating retroperitoneal sarcomatous tumors on biopsies. The finding of nonlipogenic pleomorphic tumor cells in WDLPS demonstrating Desmin positivity may be associated with a possibility of rhabdoblastic differentiation in DDLPS. Further study is necessary to elucidate this association.

ID# 45

Title: Foamy Cell Variant of Pancreatic Neuroendocrine Neoplasm Mimicking Lipid-Laden Macrophages on Small Biopsy

Authors:

Georgia Huffman MD[1] , Mary Doan MD [1] , Roshan Raza MD [1,2] ,Shilpa Jain MD [1,2]

Affiliations: [1] Department of Pathology & Immunology, Baylor College of Medicine; [2] Department of Pathology, Baylor St. Luke's Medical Center

Introduction:

The foamy cell variant of pancreatic neuroendocrine tumor presents a diagnostic challenge because it lacks typical neuroendocrine features, such as nesting architecture and salt and pepper nuclei. The cells are often more diffusely arranged, the nuclei are often bland, and the cytoplasm contains lipid rich microvacuoles.

Case Presentation:

We present a case of pancreatic neuroendocrine tumor in a 63-year-old man with a history of type 2 diabetes mellitus and autoimmune hepatitis who presented with weight loss of 30 pounds in one year. He was found to have a 1.4 cm round, pancreatic head mass on CT.

Pathology:

Histologically, the mass displayed diffusely arranged cells with bland nuclei and abundant foamy, eosinophilic cytoplasm, which at low power resembled sheets of foamy macrophages. The tumor cells were positive for synaptophysin, chromogranin, CAM5.2, CDX2, and weak PAX8; cells were negative for mucicarmine, CD45, AE1/AE3, CD68, inhibin, nuclear beta-catenin and GATA3. Ki-67 index was less than 3%.

Conclusions:

The differential diagnosis for foamy and clear cells in a pancreatic biopsy is vast, and includes primary pancreatic neoplasms, such as solid pseudopapillary neoplasm and serous cystadenoma, as well as lesions from other adjacent organs, such as clear cell renal cell carcinoma. Processes with abundant xanthomatous macrophages may also enter the differential diagnosis. Unlike the clear cell variant of pancreatic neuroendocrine tumor, foamy cell variant is not associated with Von Hippel-Lindau syndrome. Foamy cell variant is prone to misdiagnosis because it lacks characteristic neuroendocrine features and mimics other lipid-rich and clear cell processes. Judicious use of immunohistochemistry is key to the diagnosis.

ID# 46

Bi-allelic RB1 and TP53 Alterations Revealed by Comprehensive Molecular Profiling in an Adolescent With Cardiac Leiomyosarcoma

Anindita Ghosh, MD, PhD[1], Kalyani R Patel, MD[1] , Norma M Quintanilla, MD[1], Nahir Cortes Santiago, MD, PhD[1], Kevin Fisher, MD, PhD[1]

1. Department of Pathology & Immunology; Baylor College of Medicine

Introduction: TP53 and RB1 inactivation are observed in more than 90% of leiomyosarcoma cases and are considered molecular hallmarks of this tumor type. However, such alterations are difficult to assess using standard NGS testing that target coding exons. The ability to employ additional comprehensive modalities to detect rare molecular alterations in "negative" cases is of significant interest to the molecular diagnostics community.

Case Presentation: The patient is a 13-year-old girl with no significant past medical history. She presented with dyspnea, orthopnea, progressive fatigue, and loss of appetite over the past six months. Echocardiography demonstrated a mass that extended from the right atrium across the tricuspid valve and into the right ventricle with associated pericardial and pleural effusions.

Pathology: Soft tissue mass from right atrium was removed and sections showed spindle cells with elongated blunt ended nuclei and inconspicuous nucleoli. Scattered spindle cells with hyperchromatic and variably pleomorphic nuclei were also identified. Immuno-histochemical analysis showed h-Caldesmon – positive, HHF35 – positive, Desmin – positive, SMA – positive, MSA – positive, CD34 – positive and TP53 – Negative. The diagnosis was rendered as Cardiac Leiomyosarcoma, (FNCLCC Grade-1). Targeted next-generation sequencing (NGS) using combined targeted DNA- and RNA-sequencing did not reveal any clinically significant alterations in coding and splicing regions of 2880 exons in 169 genes. The TERT promoter region and the chromosome 19 microRNA cluster (C19MC) region were found to be unaltered. No in frame gene fusions were detected with select exons in 81 genes. Transcriptome sequencing revealed out-of-frame fusion transcripts between 5' gene RPL21 [Ribosomal protein L21] exon 2 and 3' gene RB1 [RB transcriptional corepressor 1] exon 4 and 5' gene RB1 exon 3 and an uncharacterized lncRNA 3' gene [LOC101927668 on chromosome 7]. Cancer cytogenomic (OncoScan) microarray showed multiple copy-number alterations including an 8.2 Mb loss on 13q14.12-q14.3 (RB1), a 2.8 Mb loss on 17p13.2-p13.1 (TP53), loss of 10q (PTEN), and a 1.3 Mb bi-allelic loss of 10q22.2 (KAT6B. Additional manual review of the array data revealed a small 5' gene deletion (~0.2 Mb) involving TP53 exon 1.

Conclusions: Chromosomal losses affecting tumor suppressor genes such as *TP53*, *RB1*, and *PTEN* are major features of leiomyosarcoma, and copy-number alterations affecting epigenetic modifiers such as *KAT6B* are also frequently reported. RB1 loss-of-function fusions and various 5' TP53 gene deletions are recurrent mechanisms for RB1 and TP53 inactivation, respectively. Both the RPL21::RB1 and RB1::LOC101927668 fusions are predicted to result in an *RB1* frameshift and loss of RB1 protein function. Furthermore, copy-number analysis revealed *RB1* loss and thus together, the tumor was predicted to harbor biallelic *RB1* inactivation. Copy-number analysis detected *TP53* loss and manual review of the copy-number data revealed a *TP53* 5' gene deletion involving exon 1 consistent with a "second hit" and biallelic *TP53* inactivation. This case highlights the importance of test selection and comprehensive assessment for tumors that harbor a broad spectrum of molecular alterations.

ID# 47

Comparative Evaluation of Stool Processing Methods for Detection of *Mycobacterium tuberculosis* complex With a Commercial PCR Assay in Pediatric Specimens

Heather C. Binns[1,2], Coreen L. Johnson [1,2], Denver Niles [1,2], Jim Dunn [1,2]

[1] Department of Pathology, Texas Children's Hospital, Houston, TX
[2] Department of Pathology and Immunology, Baylor College of Medicine, Houston, TX

Introduction: Pulmonary tuberculosis (TB) in children is often paucibacillary which poses significant challenges for rapid and accurate diagnosis. Sputum is unlikely to be obtained from young children, so alternative specimen types that are invasive and costly to obtain, such as nasal gastric aspirates and bronchoalveolar lavage specimens, are currently used. As an alternative, the WHO endorses stool as a non-invasive specimen for pediatric TB diagnosis with rapid, molecular diagnostic platforms such as the Xpert® MTB/Rif (Cepheid, Sunnyvale, CA). However, there is a lack of agreement in the field regarding stool processing techniques, with a variety of protocols, materials, and levels of technologist expertise needed for the diverse techniques reported. We evaluated two processing methods for clinical diagnostic utilization of the Xpert® MTB/Rif assay with pediatric stool specimens.

Methods: A total of 34 contrived stool samples were processed using either gravity sedimentation or centrifugation methods prior to performing the Xpert® MTB/Rif assay. For all methods, approximately 1 gram of semi-solid stool (Bristol score 5 or 6) was inoculated with known concentrations ($\geq 10^3$ cells/g) of MTB DNA (MMCQI, Saco, ME). Samples were then mixed thoroughly with 10 mL of 1X PBS, either by vortexing or manual shaking, and left to stand upright for 15 minutes to allow heavier particles to settle. Two milliliters of supernatant was combined with 2mL Xpert® MTB/Rif Sample Reagent and incubated for 15 minutes before adding the processed sample to the cartridge and performing the assay. For the centrifugation method, the same protocol was used except the supernatant obtained after settling was centrifuged at varying speeds (500, 1000, 1500, and 2500 x g) for 10 minutes. The supernatants following centrifugation were then combined with Sample Reagent and tested with the assay.

Results: Centrifugation processing methods for stool specimens resulted in an invalid rate that was threefold less than sedimentation alone using the Xpert® MTB/Rif assay (61.5% (8/13) by sedimentation alone vs 19.0% (4/21) with the addition of centrifugation). All invalid runs for the centrifugation processing method were contrived from the same original specimen centrifuged at 500 x g (4/8) while there were no invalid runs (0/7) with samples processed with 1000 x g centrifugation speed.

Conclusions: Stool is a challenging specimen for nucleic acid amplification by the Xpert® MTB/Rif assay. The addition of centrifugation after mixing stool specimens has the potential for fewer invalid results.

ID# 49

A Single Cell Genomics Atlas of the *Drosophila* Larval Eye Reveals Distinct Clusters Corresponding to All Major Cell Types

Komal Kumar Bollepogu Raja[1], Kelvin Yeung[1], Yumei Li[2], Rui Chen[2], Graeme Mardon[1,2]

[1]Department of Pathology and Immunology, Baylor College of Medicine, One Baylor Plaza, Houston, Texas 77030, USA

[2]Department of Molecular and Human Genetics, Baylor College of Medicine, One Baylor Plaza, Houston, Texas 77030, USA

Introduction

The *Drosophila* eye is a powerful model system to study the dynamics of cell differentiation, cell state transitions, and pattern formation. Many genes and signaling pathways involved in retinal determination, such as *Pax6* (*eyeless* in flies), are highly conserved between humans and flies and are required for eye development in both species. Therefore, the eye has served as an important system for characterizing these pathways. The adult eye is a highly organized hexagonal crystal lattice, and any perturbation caused by genetic alteration can be easily scored in living animals, rendering it one of the most powerful tools for genetic screens in higher eukaryotes. Furthermore, gene function can be readily tested in the eye without causing lethality as the eye is not required for survival. In addition, given the availability of an extensive set of tools for genetic manipulation, the *Drosophila* eye has served as a prominent human disease model, particularly for neurodegenerative diseases such as Alzheimer, Parkinson, and Huntington disease. The adult eye develops from a neuro-epithelial sac during the late second instar larval stage. In the larval eye disc, the cells are arranged in a developmental space-time continuum with more mature differentiating and progenitor cells found toward the posterior of the eye disc while less mature uncommitted progenitor cells are located anteriorly, poised to undergo differentiation. This progressive, temporal component is a unique aspect of larval eye development compared to most other *Drosophila* tissues. Since the *Drosophila* eye is an important experiment model, a high-resolution single cell genomics resource that accurately profiles all major cell types of the larval eye disc and their spatiotemporal relationships is required and is currently lacking.

Methods

We extracted single cells (RNA) and nuclei (chromatin) from *Drosophila* late larval eye discs and generated libraries using the 10x Genomics platform. Both single cell RNA (scRNA) and single nuclear assay for transposase accessible chromatin (snATAC) sequence data were normalized, scaled and reduced. We profiled 26,999 cells for scRNA-seq and 20,034 snATAC-seq.

Results

We present transcriptomic and chromatin accessibility data for all known cell types in the developing late larval eye disc. Our data show all expected cell types in the late larval eye disc and all clusters are unambiguously identified and distinct from one another. Remarkably, each cell cluster in our dataset exhibits a temporal component that closely correlates with the developmental progression of cell differentiation in the physical eye disc. The photoreceptor

– continued on page 61

– *continued from page 60*

subtypes appear as thin strands of cells that represent their dynamic developmental timelines. In addition, as photoreceptors mature, they appear to assume a common transcriptomic profile that is dominated by genes involved in axon function. We identify several cell type-specific maturation genes, enhancers, and potential regulators of eye function.

Conclusion

We report a comprehensive high quality single cell genomics atlas of the developing *Drosophila* late larval eye disc. Our single cell data will greatly aid research groups studying different aspects of early eye development and will facilitate a deeper understanding of the larval eye as a model system.

References

1. Bollepogu Raja, K.K., Yeung, K., Shim, YK. *et al.* A single cell genomics atlas of the *Drosophila* larval eye reveals distinct photoreceptor developmental timelines. *Nat Commun* **14**, 7205 (2023). https://doi.org/10.1038/s41467-023-43037-0

ID# 52

COP1 Regulation of AR Signaling and Prostate Cancer Therapy Resistance

Tao Shen[1], Bingning Dong[2], Feng Yang[1]

[1]Department of Pathology & Immunology, [2]Department of Medicine, Baylor College of Medicine

Introduction: Androgen receptor (AR) signaling, central to prostate development and homeostasis, becomes dysregulated in prostate cancer, driving tumorigenesis and therapeutic resistance. Androgen deprivation therapy (ADT) is initially effective in most AR^+ advanced/metastatic prostate cancer. However, patients inevitably develop lethal castration-resistant prostate cancer (CRPC) that also resists the next-generation AR signaling inhibitors. Most CRPCs express AR; attacking AR signaling activation remains a major therapeutic approach for CRPCs. GATA2, a transcription factor involved in various developmental processes, has been implicated in prostate cancer pathogenesis through its interaction with AR and modulation of androgen-responsive genes. The interplay between AR and GATA2 orchestrates a complex regulatory network governing prostate cancer cell proliferation, survival, and metastasis. Docetaxel-based chemotherapy initially elicits favorable responses in many CRPC patients. However, patients eventually develop resistance, leading to disease progression and therapeutic failure. GATA2 has emerged as a key player in mediating resistance to docetaxel in prostate cancer. Hence, targeting GATA2/AR signaling presents a promising avenue for therapeutic intervention in prostate cancer. While directly inhibiting GATA2 transcriptional activity remains challenging, enhancing GATA2 degradation is a plausible therapeutic strategy. How GATA2 protein stability is regulated in prostate cancer remains unknown.

Methods: Various human PCa/CRPC cell lines were engineered with overexpression or knockdown of COP1 and other targets. Western blot and qRT-PCR were used to assess gene expression and signaling cascades. Co-IP and GST pulldown assays were applied to detect protein interaction. Cell proliferation and soft-agar colony formation assays were utilized to

– continued on page 63

– *continued from page 62*

determine cell growth including anchorage-independent growth in vitro. Xenograft studies were performed to assess human PCa/CRPC cell-derived tumor growth in vivo.

Results: We identify that COP1, an E3 ubiquitin ligase, drives GATA2 ubiquitination at K419/K424 for degradation. GATA2 lacks a conserved [D/E] (x)xxVP[D/E] degron but uses alternate BR1/BR2 motifs to bind COP1. By promoting GATA2 degradation, COP1 inhibits AR expression and activation and represses prostate cancer cell and/or xenograft growth, castration resistance, and docetaxel resistance. Accordingly, GATA2 overexpression or COP1 mutations that disrupt COP1-GATA2 binding block COP1 tumor-suppressing activities.

Conclusion: We conclude that GATA2 is a major COP1 substrate in prostate cancer and that COP1 promotion of GATA2 degradation is a direct mechanism for regulation of AR expression and activation, prostate cancer growth, castration resistance, and docetaxel resistance.

ID# 53

Metachronous Atypical Parathyroid Tumor and Multiple Foci of Ossifying Fibroma in Hyperparathyroidism Jaw-Tumor (HPT-JT) Syndrome – A Recurrent Case with Diagnostic Pitfalls

Dorsay Sadeghian[1], Angela Haskins[2], Wendong Yu[3], Ya Xu,[1,4]

[1] Department of Pathology & Immunology, Baylor College of Medicine, Houston, TX 77030

[2] Department of Otolaryngology-Head and Neck Surgery, Baylor College of Medicine, Houston, TX 77030

[3] Department of Pathology & Laboratory Medicine, MD Anderson Cancer Center, Houston, TX 77030

[4] Department of Pathology & Laboratory Medicine, Ben Taub Hospital, Harris Health System, Houston, TX 77030

Introduction:

Atypical parathyroid tumor (APT) is uncommon and may occur in familial syndromes. We report a case of recurrent hyperparathyroidism jaw-tumor (HPT-JT) syndrome with metachronous APT and multiple ossifying fibromas, highlighting diagnostic pitfalls.

Case Presentation:

This was a 20-year-old male who presented with bone pain and blurry vision previously diagnosed with HPT-JT syndrome and a left APT harboring *CDC73* gene germline mutation at outside hospital 9 years prior. Imaging displayed a right inferior parathyroid mass (1.1 cm) and multiple osseous lesions in the right maxilla (4.5 cm), right mandible (1.3 cm), left mandible (0.9 cm). He underwent parathyroidectomy and biopsies of the larger osseous lesions.

Pathology

Microscopic examination of the parathyroid mass revealed a partially encapsulated parathyroid neoplasm adherent to the thymus. The tumor was arranged in trabeculae and sheets with fibrotic bands. Focal moderately pleomorphic tumor cells extended into the remaining parathyroid gland. Immunohistochemistry demonstrated loss of parafibromin expression. These features of the tumor were suspicious, but not sufficient, for a malignant diagnosis. The osseous lesions consisted of fibrous proliferation and bony tissue. The histologic findings of the fibrous component resembled solitary fibrous tumor, but with negative STAT6 immunostain and reduced parafibromin expression. Final diagnoses of APT and multiple ossify fibromas were rendered.

Conclusion:

The parathyroid neoplasms in HPT-JT syndrome usually involve only one parathyroid gland. In this case, the metachronous APTs involve two parathyroid glands. The APT displays loss of parafibromin expression with histologic features mimicking parathyroid carcinoma, and the fibrous components of ossifying fibromas resemble solitary fibrous tumor, highlighting diagnostic pitfalls.

ID# 54

Enhancing Pathogen Detection and Characterization of Respiratory Microbiome Signatures of Infection Through Next-Generation Sequencing

Per A. Adastra[1,2], Angela V. Serrano[1,2], Jessica K. Runge[1,2], Michelle Leeman [1,2], Michelle Rubio-Gonzales [1,2], Marudhu P. Murugesan[1,2], Jennifer K. Spinler[1,2], and Ruth Ann Luna[1,2]

[1] Department of Pathology & Immunology, Baylor College of Medicine, Houston, Texas, USA; [2] Texas Children's Microbiome Center, Department of Pathology, Texas Children's Hospital, Houston, Texas, USA

Introduction

Next-generation sequencing-based (NGS) methods offer a comprehensive view of the microbial makeup in clinical samples and are used strategically in parallel to culture-based methods. While NGS-based methods cannot confirm organism viability, culture-based methods can but are limited by the number of culture conditions routinely utilized in clinical microbiology laboratories. Conversely, the wide scope of NGS-based methods addresses these limitations but introduces challenges in differentiating actual pathogens from expected body-site-specific microbiome or benign transient colonizers. This study evaluates the effectiveness of NGS for identifying pathogens in respiratory samples, comparing it with the existing diagnostic approaches at Texas Children's Hospital in Houston, Texas, which includes culture-based assays, targeted PCR assays, and sequencing performed by reference laboratories. We hypothesize that employing sample metadata (source, type, etc.) and patient data (clinical history, chronic conditions, etc.) during data analysis will help distinguish pathogens from expected flora in respiratory samples.

Methods

To develop these methods, 27 respiratory samples with sufficient volume for both routine diagnostic testing and this study were collected. Nucleic acid was extracted using the Qiagen DNeasy PowerSoil Pro Kit after collection, and targeted short-read sequencing (16S, 18S/ITS) was performed. These data were then analyzed using a custom bioinformatic pipeline built around Qiime2-2022. In brief, sequences are denoised and quality-filtered using DADA2, an algorithm that uses a statistical model for correcting sequencing errors, after which similar amplicon sequence variants (ASVs) are clustered. Next, a feature table of ASVs that are 100% identical is generated, and taxonomy is assigned using a naive Bayes taxonomy classifier against the Silva 13.2 database. Finally, unassigned and low-abundance ASVs are removed. When species-level identification could not be determined through targeted short-read sequencing, untargeted long-read sequencing was used.

Results

In one case, we found that a bronchoalveolar lavage sample from the lung of a patient with a history of recurrent pneumonia contained a singular pathogenic bacterium, *H. influenzae.* This finding agreed with results obtained through reference laboratory-generated sequencing. In another case, we identified >14 unique bacteria at varying concentrations in a wash sample collected from the lung of an asymptomatic patient during a routine bronchoscopy. These findings, however, were determined to be expected respiratory flora.

Conclusions

Our NGS-based methods improve pathogen detection compared to current diagnostics by discriminating between respiratory flora and active infections. Setting thresholds for pathogen detection, evaluating clinical relevance in the context of body site and presentation, and deploying additional molecular techniques when necessary are crucial steps to increase the accuracy of pathogen detection in the clinic.

ID# 55

Title:

AMER1 Copy Loss as an Alternative Mechanism for Wnt-Pathway Activation in High-Risk Pediatric Malignant Hepatocellular Tumors

All Authors:
Cagla Yasa Benkli, Baylor College of Medicine **(Primary Presenter)**
Stephen F. Sarabia, Baylor College of Medicine/Texas Children's Hospital
Martin Urbicain, Baylor College of Medicine/Texas Children's Hospital
Kevin E Fisher, Baylor College of Medicine/Texas Children's Hospital
Pavel Sumazin, Baylor College of Medicine/Texas Children's Hospital
Kalyani Patel, Texas Children's Hospital
Dolores Lopez-Terrada, Texas Children's Hospital, Baylor College of Medicine

Background:

Pediatric malignant hepatocellular tumors, comprising hepatoblastoma(HB), hepatocellular carcinoma(HCC), and hepatocellular neoplasm, NOS(HCN NOS) are rare tumors with incidence ~ 5 cases/million/year in US. Majority are Wnt pathway activated due to mutations in *CTNNB1*, and rarely in other genes such as *APC* and *AXIN1*. Herein, we report the clinicopathological features alongside genomic and expression profiling of 3 *CTNNB1* wild-type, high-risk(HR) pediatric hepatocellular tumors carrying *AMER1* intragenic deletions or truncating variants, as an alternative mechanism for Wnt pathway activation.

Design:

AMER1 copy loss was detected by Affymetrix Oncoscan SNP array in 3 of 168 (1.8%) clinically and histologically annotated liver tumors collected by our institution since 2003. Molecular features were evaluated with mutation profiling with a 124-gene NGS panel and by mRNA expression analysis with a NanoString PanCancer panel.

Results:

Patients with liver tumors carrying *AMER1* defects (2M, 1F; age 10-16 years) showed either combined (n=2) or overlapping histological features(n=1) of HB and HCC(HCN NOS). Case 1 and 3 had significant intra-tumor heterogeneity, including areas of fetal HB with high mitotic index, embryonal pattern and undifferentiated areas arranged in solid and macrotrabecular patterns. Case 2 showed acinar/macrotrabecular patterns with intermediate cytology. Significant pleomorphism was present in all tumors and background liver was normal in all. CHIC

– continued on page 67

– *continued from page 66*

risk stratification was HR with at least one HR feature of portal vein invasion, multifocality or PRETEXT 4. By NGS, the female patient carried a second hit to *AMER1*, a p.Glu251Ter pathogenic variant plus an *ARID1A* frameshift variant. Patient 3 had a 9 bp del in *ATM*. A high degree of genomic instability was observed with copy gain of 1q, 2q, 5, 6p, 7, 8q, 10q, 12, 19, 20, 21 and 22 in all cases. mRNA expression profiling detected reduced*AMER1* expression and Wnt pathway activation in all. Other HR biomarkers included copy gain of *MDM4*, copy loss of *CDKN2A* and reduced p53 activity.

Conclusion:

Clinicopathological characterization of pediatric liver tumors carrying *AMER1* alterations, confirms *AMER1* inactivation as an alternative mechanism for Wnt pathway activation in these rare tumors. Histological features and copy number abnormalities are consistent with those in high-risk tumors in the HB/HCN, NOS group. The presence of *AMER1* inactivation, might be helpful in the diagnosis and potentially to risk stratify these challenging cases.